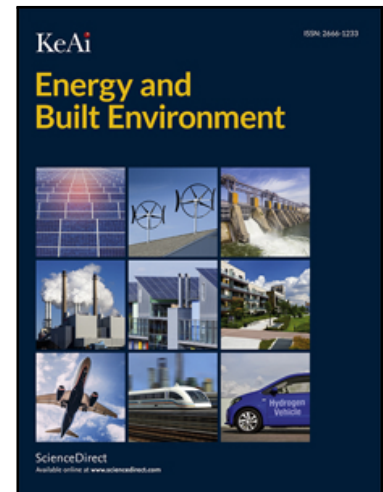


Journal Pre-proof

Detecting the Changing Impact of Urbanisation on Urban Heat Islands in a Tropical Megacity Using Local Climate Zones

Tania Sharmin , Adrian Chappell

PII: S2666-1233(25)00014-5
DOI: <https://doi.org/10.1016/j.enbenv.2025.02.002>
Reference: ENBENV 380



To appear in: *Energy and Built Environment*

Received date: 17 August 2024
Revised date: 4 February 2025
Accepted date: 5 February 2025

Please cite this article as: Tania Sharmin , Adrian Chappell , Detecting the Changing Impact of Urbanisation on Urban Heat Islands in a Tropical Megacity Using Local Climate Zones, *Energy and Built Environment* (2025), doi: <https://doi.org/10.1016/j.enbenv.2025.02.002>

This is a PDF file of an article that has undergone enhancements after acceptance, such as the addition of a cover page and metadata, and formatting for readability, but it is not yet the definitive version of record. This version will undergo additional copyediting, typesetting and review before it is published in its final form, but we are providing this version to give early visibility of the article. Please note that, during the production process, errors may be discovered which could affect the content, and all legal disclaimers that apply to the journal pertain.

Copyright © 2025 Southwest Jiatong University. Publishing services by Elsevier B.V. on behalf of KeAi Communication Co. Ltd.

This is an open access article under the CC BY license (<http://creativecommons.org/licenses/by/4.0/>)

Highlights

- Natural areas are 2.4°C and 1.3°C cooler than compact and open areas, respectively.
- Open low-rise, mid-rise and high-rise built areas are most suitable for Dhaka.
- No statistical LST differences between compact and large low-rise built areas.
- NDVI properties of compact and heavy industry are statistically identical.

Journal Pre-proof

Detecting the Changing Impact of Urbanisation on Urban Heat Islands in a Tropical Megacity Using Local Climate Zones

Tania Sharmin ^{*,1} and Adrian Chappell²

*Corresponding author

1 - Welsh School of Architecture, Cardiff University, Cardiff, United Kingdom. Email: SharminT@Cardiff.ac.uk

2 - School of Earth and Environmental Sciences, Cardiff University, Cardiff, United Kingdom.

Email: chappella2@cardiff.ac.uk

Abstract

This study integrates urban morphology-based heat island estimates with Local Climate Zone (LCZ) classifications, a methodology that is relatively underexplored in the context of tropical megacities. We use Land Surface Temperature (LST), and Normalised Difference Vegetation Index (NDVI) measured from satellite data to establish the differences across the LCZ classes and to identify suitable climate-sensitive built-environments for the megacities. High-density built-up areas had higher LSTs and Surface Urban Heat Island (SUHI) estimates than areas with more vegetation. When comparing average summer LSTs in built-up areas, areas with higher building density and minimal vegetation cover were 1.2°C warmer than the more open built environments. Natural areas, on the other hand, showed an average LST that was 2.4°C cooler than the compact built environment and 1.3°C cooler than the open built environment. For tropical megacity Dhaka, open low-rise, mid-rise and high-rise morphology emerges as more favourable built environment benefiting both people and the local biodiversity. Conversely, areas comprising compact mid-rise, large low-rise and heavy industry buildings that are becoming increasingly densely populated, are the least suitable options. Given the increasing need for high-density living, our results indicate that the most suitable approach to planning would be to substitute compact low-rise housing, typically prevalent in developing country megacities as slums, with a combination of open high-rise and open mid-rise housing. This study demonstrates that increasing SUHI and LSTs can be mitigated in densely populated tropical megacities by appropriate planning using urban morphology as demonstrated by LCZ classification.

Keywords

Land Surface Temperature, Vegetation Indices, Local Climate Zone Classification, Urban Heat Island, Tropical Megacities.

1. Introduction

Urbanisation often fosters urban growth through the expansion of industry, transportation and economic activity [1]. However, in developing countries rapid population growth often precedes the essential infrastructure and services needed to support urbanisation leaving the urban populations highly susceptible to the impacts of climate change [2]. The average annual air temperature in large cities with over one million population may increase up to 1-3°C compared to the surrounding non-urban areas [3], [4]. Megacities with over 10 million inhabitants experience rapid and often unplanned urbanisation. The combination of high population density and lack of resources and infrastructure can have a more devastating effect on the overall well-being of the population. People's vulnerability to adverse climate impacts is exacerbated by heat stress [5], [6] and infectious diseases sensitive to climate conditions [7]. Such large magnitudes of population in megacities directly influence Land Use Land Cover (LULC) changes, and the local microclimate, which in turn influences the regional climate through physical processes like heat flux, wind speed, and boundary layer turbulence [8]. Therefore, it is crucial to understand the mechanism of interaction between LULC change and local microclimate for building resilience and enhancing adaptability in mitigating climate impacts.

Despite the recognised impact of the built environment's influence on urban climate, a gap persists in applying this knowledge to guide policymakers in urban planning and Land Surface Temperature (LST) management. This study seeks to bridge this gap by focusing on the unique challenges of a megacity context, integrating Urban Heat Island (UHI) observations with analyses of LST and built morphology. Key challenges include the absence of systematic criteria for evaluating design and communicating UHI effects, and inconsistent depiction of city characteristics [9]. These limitations obscure the spatial correlation between urbanisation and urban climate change within cities.

Urbanisation transforms the local climate by increasing air temperature and LST [10] leading to UHI. Urban areas experience higher temperatures compared to their surrounding rural areas [4], caused by increased anthropogenic activities, artificial surfaces, and alteration of the natural environment. To address the spatial vulnerability of the urban population in high-density cities, it is important to consider the combined effect of urban micro-climate change and the urbanisation process for individual cities.

The Urban Heat Island (UHI) effect is a global phenomenon with severe implications for megacities in developing countries, particularly in the tropics, where the extreme high-density urban form is compounded by limited resources for adequate housing, green infrastructure, and essential urban amenities. The UHI can be explained by two phenomena: the Atmospheric Urban Heat Island (AUHI); the Surface Urban Heat Island (SUHI). The assessment of the AUHI involves evaluating the air temperature patterns in urban and rural areas through field measurements, while the SUHI

relies on LST. Although AUHI can be successfully examined by actual measurements of air temperatures, this is

always the most feasible way to collect data often leading to difficulties in conducting large-scale and long-term research [8]. Alternatively, researchers often rely on data collected at meteorological stations. However, the availability of meteorological stations is generally limited in developing countries. Therefore, the use of LST retrieved from infrared remote sensing imagery is a cost-effective and consistently reliable approach to understand the spatial pattern of SUHI in an urban area which can provide continuous data for an entire city.

Recent studies have shown a strong association between LST and air temperature highlighting the benefits of using satellite-based LST as an alternative for air temperature in regions where meteorological data are scarce [11]. However, some researchers point out limitations in satellite remote sensing methods, which use directional instruments to measure LSTs from a specific angle, primarily capturing urban surfaces like roads and roofs rather than vertical structures such as walls [12]. Additionally, these instruments sample from facets both inside and outside the urban canopy layer (UCL). Despite potential concerns about bi-directional reflectance, angular reflectance techniques are capable of calculating albedo [13], [14], effectively addressing some previously noted issues. Nonetheless, researchers cannot manipulate these instruments or choose the best observation times based on weather conditions. Despite these limitations, satellite-based SUHI studies provide comprehensive views of entire cities, overcoming many obstacles faced in assessing the AUHI. Their primary strength lies in providing global coverage and repeated observations over time, enabling comparisons of SUHI magnitude across multiple cities.

Another crucial point to consider is the difficulty of identifying and documenting the fast-changing pattern of the city through the conventional LULC maps which often lack in appropriate morphological and surface property details of the built-up area, particularly in developing country megacities. Limited field measurements and isolated stationary networks may not always capture the full range of thermal characteristics resulting from changes in LULC patterns [15], [16]. In this context, Local Climate Zone (LCZ) classification [17] using remote sensing data presents a novel and demonstrated approach to understanding the changing pattern of climate and its relationship with the built environment, vegetation patterns and water. This approach allows for the investigation of changes in SUHI properties over time due to rapid urbanisation and/or shifts in weather and climate. The LCZ is a standardised classification of urban climate where each classes are defined as “regions of uniform surface cover, structure, material, and human activity that span hundreds of meters to several kilometres in horizontal scale” [17]. The classification gives the urban planners/designers an opportunity to distinguish the microclimate impact resulting from different urban

structures (for example, high-rise vs. low-rise structures, high-density vs. low-density structures, dense vegetation vs. sparse vegetation etc.) to be reflected in urban planning and regulations.

Accordingly, the aim of this study is to enhance our understanding of how urbanisation affects the microclimate and provide insights for urban planning and climate management in the tropical megacity Dhaka. Specifically, this involves developing a clearer understanding of the functional relationship between urbanisation, urban morphology, and their effects on Dhaka's local microclimate. The objectives are to investigate how rapid urbanisation influences the local climate, evaluate the role of local climate classification in explaining microclimate variations, and identify the LCZs in Dhaka that experience the greatest and least impact.

To achieve these aims, the study employs a comprehensive approach, utilising an LCZ map and remote sensing data to extract key parameters such as LST, NDVI and SUHI intensities. This methodological framework is designed to provide a detailed analysis of the interconnections between urban growth and climatic changes in Dhaka.

The structure of the paper is designed to provide a thorough understanding of urbanisation's effects on urban climate, with a focus on SUHI and LST in Dhaka, categorised by LCZ. The introduction outlines the research context and underscores the significance of addressing urban heat islands in tropical megacities. The methodology section details the tools and data sources, including LCZ mapping and satellite data for analysing temperature and vegetation. Findings on how urban morphology and vegetation impact microclimates are presented in the results section, supported by statistical analysis. The discussion section places these findings within the broader context of urban planning and policy, highlighting their implications for sustainable development. The paper concludes by summarising the key contributions and proposing future research directions, with each section building logically on the previous to highlight the study's innovation and relevance to urban environmental management.

2. Materials and Methodology

2.1. Background

Dhaka (Figure 1a) is one of the fastest growing megacities in the world with a total population of 21.7 million [18]. Population density in dense areas like slums is around 220,246 persons per square kilometre ([19], cited in [20]). In low-density areas such as non-slums, the population is around 29,857 persons per square km ([21], cited in [20]). The alteration of the LULC pattern through the expansion of urban areas resulting from rapid population growth is a significant factor contributing to climate change [1]. Accordingly, Dhaka is facing rapid and unplanned urbanisation causing significant environmental damage that poses a severe public health risk. The city's green areas are

rapidly decreasing to accommodate the increasing housing need causing air temperature to elevate and making the UHI impacts worse. Between 2000 and 2019, Dhaka's daytime SUHI increased by 0.98°C [22] with an increasing SUHI severity while the whole country has been enduring immense heatwaves in recent years [23]. The recent Dhaka Area Plan (DAP) [24], published by RAJUK (the Capital Development Authority of the Government of Bangladesh), outlines long-term plans to convert the flood-flow zones into built-up areas to mitigate the housing crisis, which may exacerbate ecological impacts. The flood-flow-zones around Dhaka play a crucial role in the regulation of the city's microclimate. They allow unobstructed flood-flow into the rivers and enable sustainable drainage but also offer adequate pervious surfaces. These surfaces reduce the impact of extreme heat and ameliorate the effect of surface energy balance compared to impervious surfaces. Studies [25] [26] have shown that flood-flow-zones, high-value agricultural land and retention ponds have decreased. From 1967 to 2010, permanent wetland reduced from 14% to 4% [27]. The DAP provides detailed implementation guides incorporating policies, guidelines and framework for the development of different areas of the city. The publication of DAP has raised serious concerns among the urban experts, environmentalists and civil society groups. Similar to the previous master plans [28], the DAP does not adequately address the effects of climate change, unplanned urbanisation on flood-flow-zones, drainage congestion and loss of biodiversity. In addition to permitting building in the flood-flow-zones as prescribed in the DAP, RAJUK also plans to legalise the already filled-up flood-flow-zones by the real-estate developers [24]. To protect Dhaka from additional damage immediate attention to these plans are required from experts and policymakers before implementation. Further details on the area plan and flood-flow zones and SUHI in Dhaka are provided in Appendix 1.

2.2. Topography and Climate of Dhaka

The elevation of Dhaka ranges from 2 to 13 metres above sea level with most urban areas at an elevation of 6-8 m [29]. According to a Japan International Cooperation Agency (JICA) Report [30], Dhaka only has 20 km² which is 8 metres above sea level, around 75 km² between 6-8 metres above sea level and 170 km² above sea level 6 metres. The city is mostly surrounded by wetlands with the Balu and Shitalakhya rivers flowing in the east, Turag River in the west, Tongi Canal in the north and Buriganga River in the south. Most land expansion is occurring in the eastern and northern fringes of the city, mainly by landfilling of the flood-flow-zones.

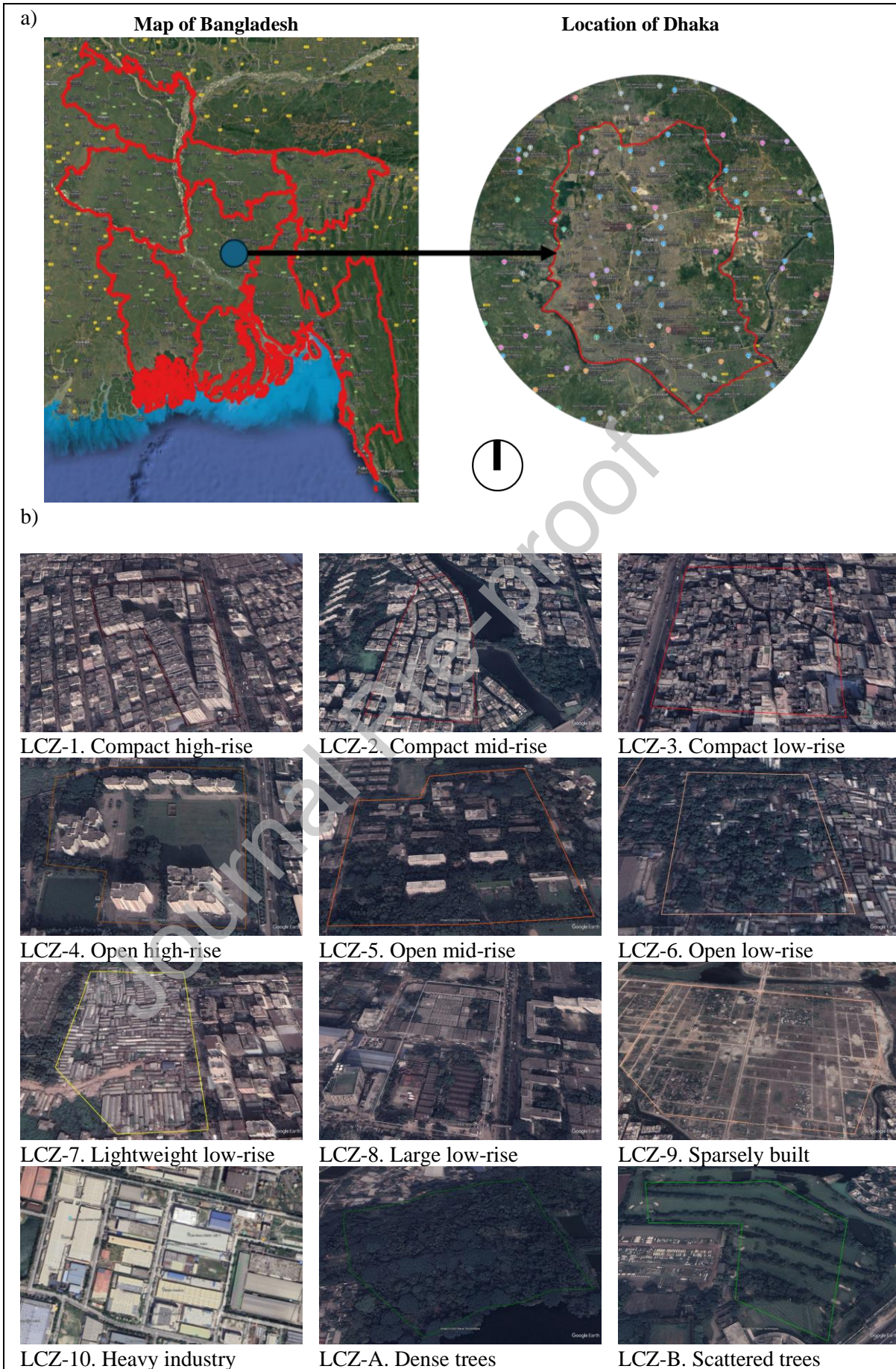
Dhaka has a tropical 'savanna' (hot-humid) climate following the Köppen climate classification. The three main seasons in Dhaka are the pre-monsoon hot season (hot-dry, from March-May), the monsoon season (hot-humid, from June-October) and a brief cool-dry season (from December-February). According to the EPW (EnergyPlus Weather) data for Dhaka, the mean annual temperature is 25.8°C with an annual range between 39.4°C to 8.2°C . April is the hottest month with

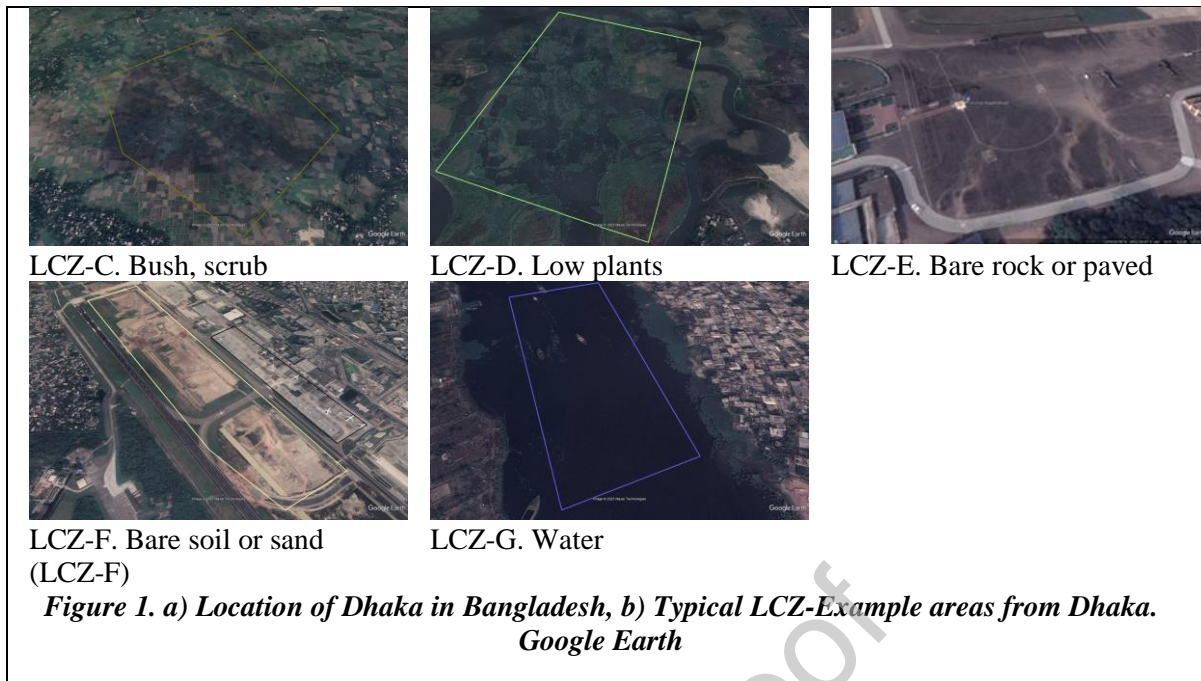
average maximum temperatures exceeding 37.5°C while January is the coolest with a mean monthly temperature of 18.5°C. The mean annual relative humidity is 75%. The mean hourly wind speed remains well below 4 m/s, with occasional gusts reaching up to 14 m/s. Dhaka receives a significant amount of solar radiation throughout the year with the average hourly maximum solar radiation exceeding 800 W/m² for almost 60% of the year.

2.3. Local climate zones of Dhaka

Previous studies [31] show high air temperature profiles across the built-up local climate zones (LCZ) in Dhaka which included microclimate measurements in Compact high-rise, (commercial, LCZ-1), Compact mid-rise, (formal and traditional residential areas, LCZ-2) and Open mid-rise (university campus, LCZ-5) areas. The average air temperature across the areas was 31.7°C during the measurement campaign with a daytime air temperature range between 27.0°C to 33.6°C. A daytime AUHI up to 2.0°C was found in LCZ-1 and formal LCZ-2, whereas traditional LCZ-2 and LCZ-5 areas showed a negative AUHI up to -1.8°C. The average air temperature in the LCZ-1, formal LCZ-2, traditional LCZ-2, and LCZ-5 were found to be 34.1°C, 32.1°C, 31.0°C and 31.1°C, respectively.

Here we extracted the LCZs for Dhaka from the Global LCZ Map developed by [32] under the World Urban Database and Access Portal Tools (WUDAPT) project. The Global LCZ Map is accessible for free download from this link: <https://zenodo.org/records/6364594>. The global map is developed using global random forest models and various earth observation data sources, including Landsat 8, Sentinel-1 and 2, PALSAR, VIIRS. It has a 100-meter resolution and demonstrates satisfactory accuracy comparable to city-specific mapping. Several studies [33]–[35] have successfully used Landsat 8 OLI/TIRS data to investigate locations of different types of LCZ. After extracting the LCZ map, it was georeferenced using the WGS 84 / UTM Zone 46 N projection system. Figure 1b includes typical example areas representing each LCZ classes in Dhaka.





2.4. Population

To examine the relationship between the population of Dhaka and LCZ classes, the spatial distribution of population data in 2020, Bangladesh was downloaded from the World Population database. The dataset available in Geotiff format at a resolution of 3 arc (approximately 100m at the equator) presents an estimated total number of people per grid-cell. Population data for each LCZ class in Dhaka is extracted using QGIS, a geographic information system (GIS) software. This involves using spatial analysis algorithms within QGIS to intersect demographic data layers with LCZ boundaries, efficiently allocating population figures to each zone.

2.5. LST

LST is an important parameter for describing microclimate conditions and is freely and globally available using satellite imagery. Since 2013, Landsat 8 satellite images have been produced every 16 days with a resolution of 30 m which allows estimation of LST from the thermal infrared sensor bands 10 and 11. Utilising Landsat-8 images is a well-established method for estimating LST and NDVI as reported in numerous studies [36]–[42].

Calculating Land Surface Temperature (LST) from Landsat-8 imagery using the thermal band 10 involves a detailed process that can be broken down into several precise steps: The first step is to calculate the spectral radiance L_{γ} from band 10. This is done using the following Equation 1 [43]. Here, L_{γ} is spectral radiance, M_L is the band-specific multiplicative rescaling factor, $QCAL$ is the quantised calibrated value in digital number (DN), and A_L is the band-specific additive rescaling factor from the metadata.

$$L_{\gamma} = M_L \times QCAL + A_L \quad \text{Equation 1}$$

The second step involves converting the spectral radiance to atmospheric brightness through the following equation. Here T_B is the top of the atmospheric brightness temperature in kelvin and K_2 , and K_1 is the band-specific thermal conversion constant of 1321.0789 and 774.8853.

$$T_B = \frac{K_2}{\ln\left(\frac{K_1}{L_{\gamma}} + 1\right)} - 271.15 \quad \text{Equation 2}$$

Step 3 is to calculate NDVI, which is essential for calculating LST for Landsat-8. Here NIR is band 5 and Red is band 4.

$$NDVI = \frac{(NIR - Red)}{(NIR + Red)} \quad \text{Equation 3}$$

Step 4 is the calculation of the proportion of vegetation using maximum and minimum NDVI.

$$P_v = \left(\frac{NDVI - NDVI_{min}}{NDVI_{max} - NDVI_{min}}\right)^2 \quad \text{Equation 4}$$

Step 5 is the calculation of land surface emissivity using P_v (55). Here, ε is emissivity.

$$\varepsilon = 0.004 \times P_v + 0.986 \quad \text{Equation 5}$$

Finally, LST values were derived from Brightness Temperature (T_B) by applying the equation from [44]. As mentioned in the reference article [44], each of the LULC categories was assigned an emissivity value by reference to the emissivity classification scheme by [45]. The calculations were performed using the Semi-Automatic Classification Plugin in QGIS [46].

$$S_t = \frac{T_B}{1 + (\lambda \times T_B / \rho) \ln \varepsilon} \quad \text{Equation 6}$$

where:

- S_t = The emissivity corrected LST
- λ = wavelength of emitted radiance (for which the peak response and the average of the limiting wavelengths ($\lambda = 11.5 \mu m$) is used.
- $\rho = h \times c / \sigma$ (1.438×10^{-2}) m K
- h = Planck's constant = (6.626×10^{-34}) J s
- σ = Boltzmann constant = (1.38×10^{-23}) J/K
- c = velocity of light = (2.998×10^8) m/s
- ε = emissivity

Table 1. Remote sensing images used in the study

<i>LANDSAT_PRODUCT_ID</i>	<i>row, path</i>	<i>Date image acquired</i>	<i>summer/ winter</i>
LC08_L1TP_137044_20210112_20210308_02_T1	44, 137	12-01-2021	Winter
LC08_L1TP_137044_20210213_20210301_02_T1	44, 137	13-02-2021	Winter
LC08_L1TP_137044_20210301_20210311_02_T1	44, 137	01-03-2021	summer
LC08_L1TP_137044_20210317_20210328_02_T1	44, 137	17-03-2021	summer
LC08_L1TP_137044_20210418_20210424_02_T1	44, 137	18-04-2021	summer
LC08_L1GT_137044_20210723_20210729_02_T2	44, 137	23-07-2021	summer
LC08_L1TP_137044_20211011_20211019_02_T1	44, 137	11-10-2021	summer
LC08_L1TP_137044_20211128_20211208_02_T1	44, 137	28-11-2021	Winter
LC08_L1TP_137044_20211214_20211222_02_T1	44, 137	14-12-2021	Winter

Analysis of LST in relation to LCZ classification is a useful tool to understand the differences across LCZ zones especially for fast-growing developing country megacities, where data is limited, and the changes are occurring rapidly. Several studies have reported significant differences in LST among different LCZ classes, confirming the applicability of LST to understanding the variability of urban form and surface properties [47][48]. In this study, nine Landsat 8 OLI/TIRS Collection 2 Level 1 (C2 L1) scenes from 2021, comprising both Tier 1 (T1) and Tier 2 (T2) data, were analysed based on data availability and quality considerations. The scenes, with a spatial resolution of 30m were downloaded from the United States Geological Survey (USGS) Landsat Data Access Portal, five for summer and four for winter, for generating LST and NDVI. Low cloud cover (less than 15%) was selected as the presence of clouds and their shadow creates misclassification due to false detection of land cover [48]. The details of the images can be found in Table 1. For comparison with the LCZ, the spatial resolutions of the images were reclassified to a spectral resolution of 100m from 30m. All spatial analyses in this study were conducted in QGIS. Statistical analysis of the data collected in this study was performed with R Programming Tool.

2.6. NDVI

Normalised Difference Vegetation Index (NDVI) is an established approach to quantify vegetation by measuring the difference between near-infrared (NIR) (strongly reflected by vegetation) and red light (absorbed by vegetation) [49] (Equation 3). Generally, healthy vegetation (chlorophyll) reflects more NIR, and green light compared to other wavelengths and absorbs more red and blue light. NDVI always ranges from -1 to +1 but does not present a distinct boundary for each type of landcover. Negative values generally indicate the presence of water, and values close to +1 would generally mean dense green, healthy leaves whereas values close to zero very likely indicate an absence of green leaves. Change in NDVI of a pixel can be caused by a change in the existing plant health (spectral greenness) but also by a change in the number of plants and vegetation cover (structure). The NDVI does not enable discrimination between spectral or structural changes. LULC changes can significantly affect vegetation type and vegetation density [8]. Therefore, it is important

to examine NDVI in relation to LCZ classes to identify the possible changes and effects. Smaller relative NDVI and density of vegetation can mean vegetation growth is impacted by water deficiency, thus identifying the signs of drought. In this study, NDVI was generated using the Semi-Automatic Classification Plugin on QGIS [46] using Landsat data. The scenes were then resampled from 30 to 100m to match the LCZ map.

2.7. SUHI

The Surface Urban Heat Island (SUHI) effect is commonly defined as the surface temperature difference between urban and rural areas [50][51][52]. The LCZ classification scheme has been proven to be an effective tool for quantifying the SUHI effect [53]. However, while SUHI signifies the surface temperature variance between urban and rural zones, LCZ does not differentiate between these two types of areas. In this study, we use LCZ-D (Low plants) as the reference for rural areas to calculate the SUHI across different LCZ classes, considering its representation of typical rural conditions, also applied in [54]. The changes in the SUHI is determined from the following equation [55]:

$$SUHI_i = \frac{T_i - T_{mean}}{T_{sd}} \quad \text{Equation 7}$$

Here, $SUHI_i$ is the pixel value of SUHI, T_i is the pixel value of LST, T_{mean} is the mean value of LST in LCZ-D and T_{sd} is the standard deviation of LST within the study area.

2.8. Minimum Detectable Change (MDC)

We apply the concept of *Minimum Detectable Change (MDC)* [56] to identify the difference in estimated means of our environmental property e.g., LST, NDVI and SUHI. Our hypothesis $H_0: \hat{d}_{2,1} = 0$; that is the mean difference in environmental property between various LCZ categories has stayed the same. The alternative hypothesis $H_1: \hat{d}_{2,1} > 0$ is that the average difference in in environmental property is different for the LCZ categories. The uncertainty due to reaching an incorrect conclusion is the MDC which is related to the probability of the errors on the conclusion. In other words, MDC is defined as a valid change in score that is not due to chance. The interpretation of the MDC_{95} is that it is the smallest change in a measure that can be considered real change beyond measurement error with 95% confidence. In the case of a one-sided test, where \hat{V} is an estimate of the spatial variance, MDC is calculated through the following equation:

$$\hat{d}_{2,1} = MDC = (X_{1-\alpha} + X_{1-\beta}) \left(\frac{\hat{V}_1}{N_1} + \frac{\hat{V}_2}{N_2} \right)^{0.5} \quad \text{Equation 8}$$

Here, X is a standard normal distribution and $N1$ and $N2$ are the samples at each sampling event. α (the size of the significance test) and β represent probability of false rejection and probability of false acceptance, respectively. $1 - \beta$ is the power of the test.

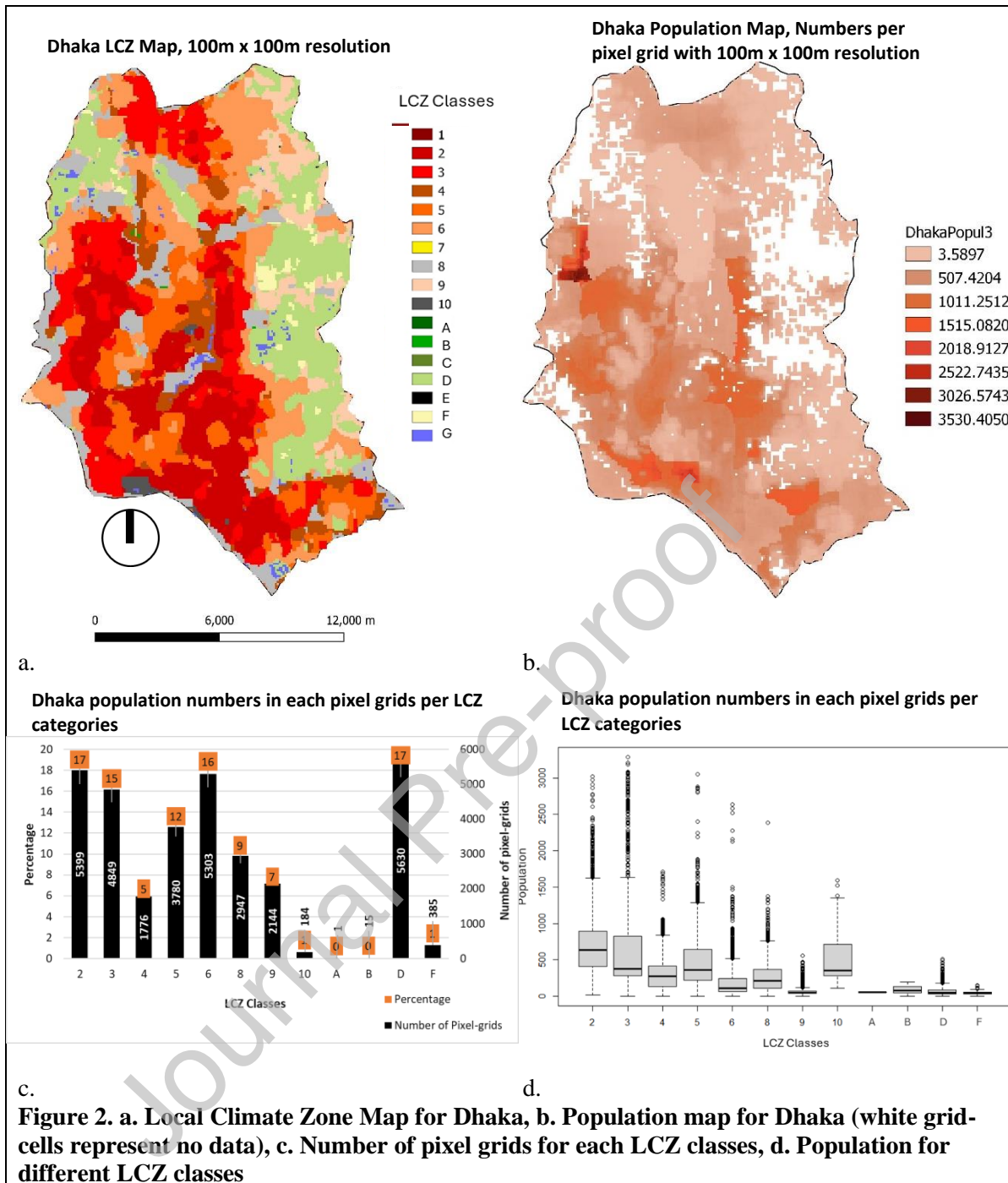
Exploring environmental differences across LCZ categories using MDC is essential. MDC offers a practical way to assess measurement error by providing a precise value for each variable in its unit of measure [57]. This value indicates the smallest change attributable to error rather than random variation or chance. In this study, MDC helps quantify the smallest statistically significant differences, enhancing our understanding of environmental impacts across urban morphologies and revealing limitations in LCZ mapping. This is crucial, as LCZ mapping often struggles to distinguish accurately between different urban morphological categories.

3. Results

3.1. LCZ Map of Dhaka and population

The primary characteristics of Dhaka's urban morphology are represented by the LCZ map (Figure 2a). The distribution of pixel grids for each LCZ class, as identified in the map, is presented in Figure 2(c). It is observed that compact built-classes cover approximately 32% of the city, while open built-classes occupy 33%. Sparsely built areas (LCZ-9) account for 7% of the city's land area, with a considerable portion situated in flood-flow zones. Large low-rise structures (LCZ-8) constitute a significant area, covering 9% of the city, while heavy industrial regions (LCZ-10) occupy 1%.

Regarding land cover classes, they are notably limited, with only 1 and 15 pixel-grids representing the LCZ-A (Dense trees) and LCZ-B (Scattered trees) categories, respectively. LCZ-D (Low plants) encompasses 17% of the city's area, but it remains negligible when compared to other megacities worldwide. Notably, LCZ-F (Bare soil or sand) covers 1% of the land, and its extent is gradually increasing due to land-filling efforts, mostly encroaching flood-flow-zones, to accommodate the city's growing population.



A limitation in the current LCZ map produced by [32] is, it does not identify the slum areas. Dhaka has more than 5,000 slums inhabited by an estimated four million people [58]. According to LCZ classification, LCZ-7 has been classified as single-story attached or detached buildings set in a compact arrangement, separated by narrow roads and alleys, and made of lightweight construction materials (thatch, wood, bamboo, corrugated metal etc.) with thin walls and roofs. This definition matches the description of slums in Dhaka. Since most slum areas in Dhaka have a dense mix of low-rise temporary structures, categorised by the [59] as jhupri (made of thatch and straw), bamboo structures, tin-shed, and others, these were expected to be grouped as LCZ-7. The study by [60]

highlighted that due to the disorganised, dense, and unregulated pattern of urbanisation, slums can produce heat hotspots posing serious health threats to the inhabitants with their intense heat exposure, poor housing conditions and reduced access to cooling. The misclassification of LCZ-7 highlights a limitation in the current LCZ map, indicating an area for improvement in future studies. Meanwhile, the omission of LCZ-1, which is typically minimal in Dhaka, along with LCZ-C (Bush, scrub) and LCZ-E (Bare rock or paved) from the current LCZ map, reflects acceptable limitations. These exclusions are justified as these categories are generally scarce in Dhaka, and their absence does not significantly impact the overall accuracy of the map.

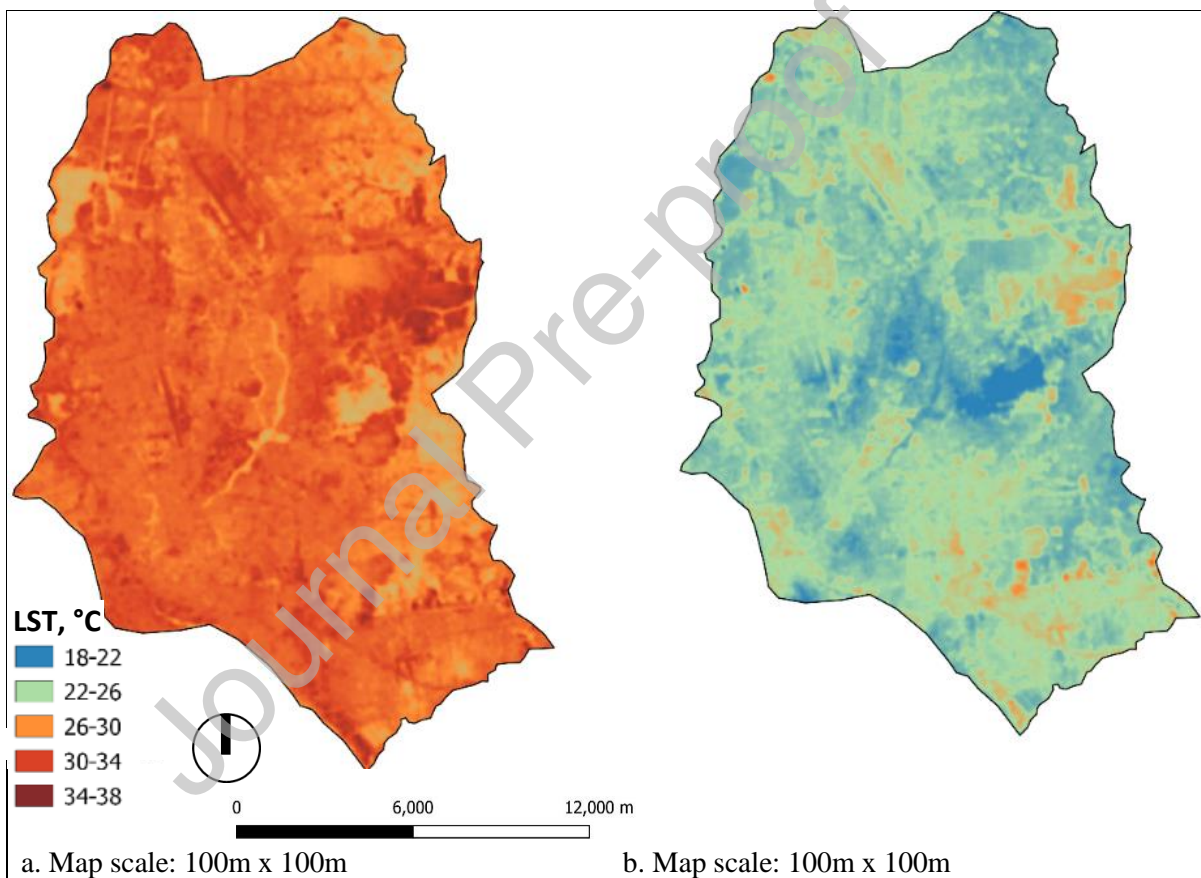
According to the population data, Figure 2b indicates that 5799 grid-cells (in white) lack data. These areas correspond to regions experiencing significant landfilling and new developments. Furthermore, the data analysis reveals that LCZ classes characterised by compact and high-density built-up areas have higher population densities. Notably, LCZ-2 (Compact mid-rise) demonstrates the highest population, while LCZ-9 (Sparsely built) exhibits the lowest population (Figure 2d). The majority of landcover classes show lower population, but some outliers are visible in LCZ-D (Low plants) and in LCZ-F (Bare soil or sand). The presence of outliers in LCZ-F is attributed to landfilling activities in flood-flow zones.

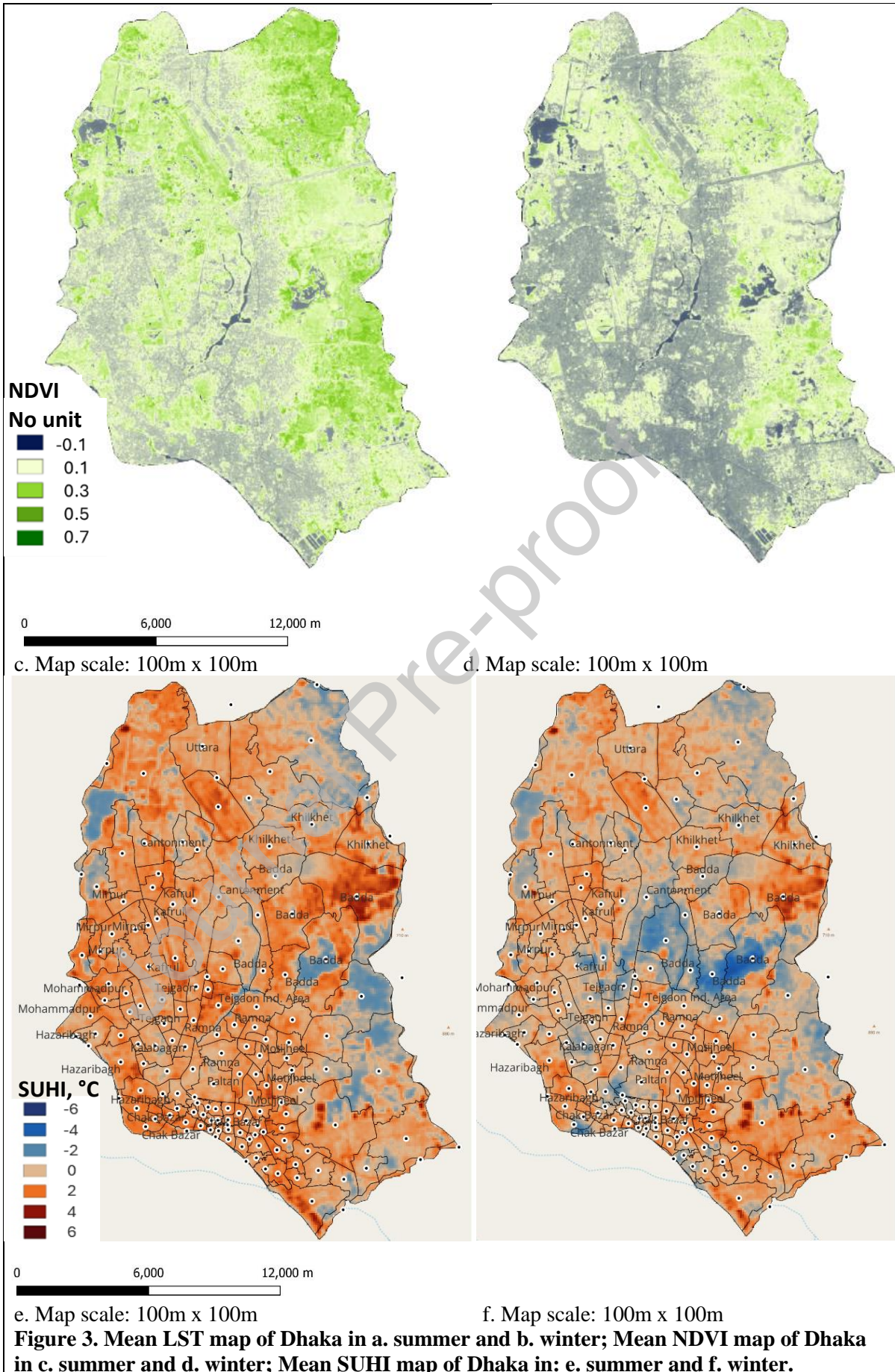
3.2. LST

The Figure 3a and Figure 3b present the mean summer and winter LSTs in Dhaka, respectively. Table 2a presents the summary statistics showing the median, minimum, and maximum values of LST. In summer, LST ranges between 23.3-37.6°C, while in winter it ranges between 15.8-31.2°C. The mean summer LST in Dhaka is on average 5.9°C higher than mean winter LST. The variation of LST throughout the year can be found in Appendix 2.

The Figure 4 and Figure 4b presents the differences in LST among different LCZs, confirming that LST can be used to distinguish between LCZ classes in urban climate studies. The LCZ classes with lower vegetation cover presented higher LST as expected. The surface physical properties and radiation balance can be highly affected by altering natural land cover by artificial land cover, consequently increasing air and surface temperatures in urban areas compared to rural areas [61]. As a result, built-up LCZ classes have higher LST than landcover classes except for LCZ-F (Bare soil and sand) with maximum summer LST of 37.6°C which has “few or no trees, plants, roads or buildings”, mostly regarded as “barren land”. Studies by [62] have also shown higher LST for LCZ-F compared to other land cover classes. Among the built-up classes, LCZ-10 (Heavy industry) has the highest median summer LST (29.2°C) which comprises “highly irregular mix of low and mid-rise industrial structures” with “few or no trees” and LCZ-9 (Sparsely built) has a lowest median LST (27.4°C) which are low-density settlements “located across natural landscape”. Similar to LCZ-10, LCZ-8 (Large low-rise) also has a considerably higher median LST (28.6°C) due to its “extensive

paved surfaces” with “few or no trees”. LCZ-2 (Compact mid-rise), 4 (Open high-rise) and 6 (Open low-rise) shows a gradual trend of decreasing LST as the amount of vegetation increases from “few or no trees” to “scattered trees and abundant plant cover” with median summer LST of 28.7°C, 27.8°C, 27.6°C, respectively. Among the compact classes LCZ-2 (Compact mid-rise) and LCZ-3 (Compact low-rise), the latter has slightly higher median LST probably due to lesser mutual shading between buildings and higher solar exposure, both resulting from urban geometry or morphological arrangements. Among the landcover classes, LCZ-A (Dense trees) has the lowest median summer LST (25.6°C) followed by LCZ-B (Scattered trees) and LCZ-D (Low plants) of 26.5°C and 27.2°C, respectively. LCZ-A (Dense trees) is omitted from further analysis due to the presence of only a single pixel-grid identified in this category on the LCZ map, suggesting that the data is not representative. In winter, LST patterns are like summer, except for the variation in magnitude.

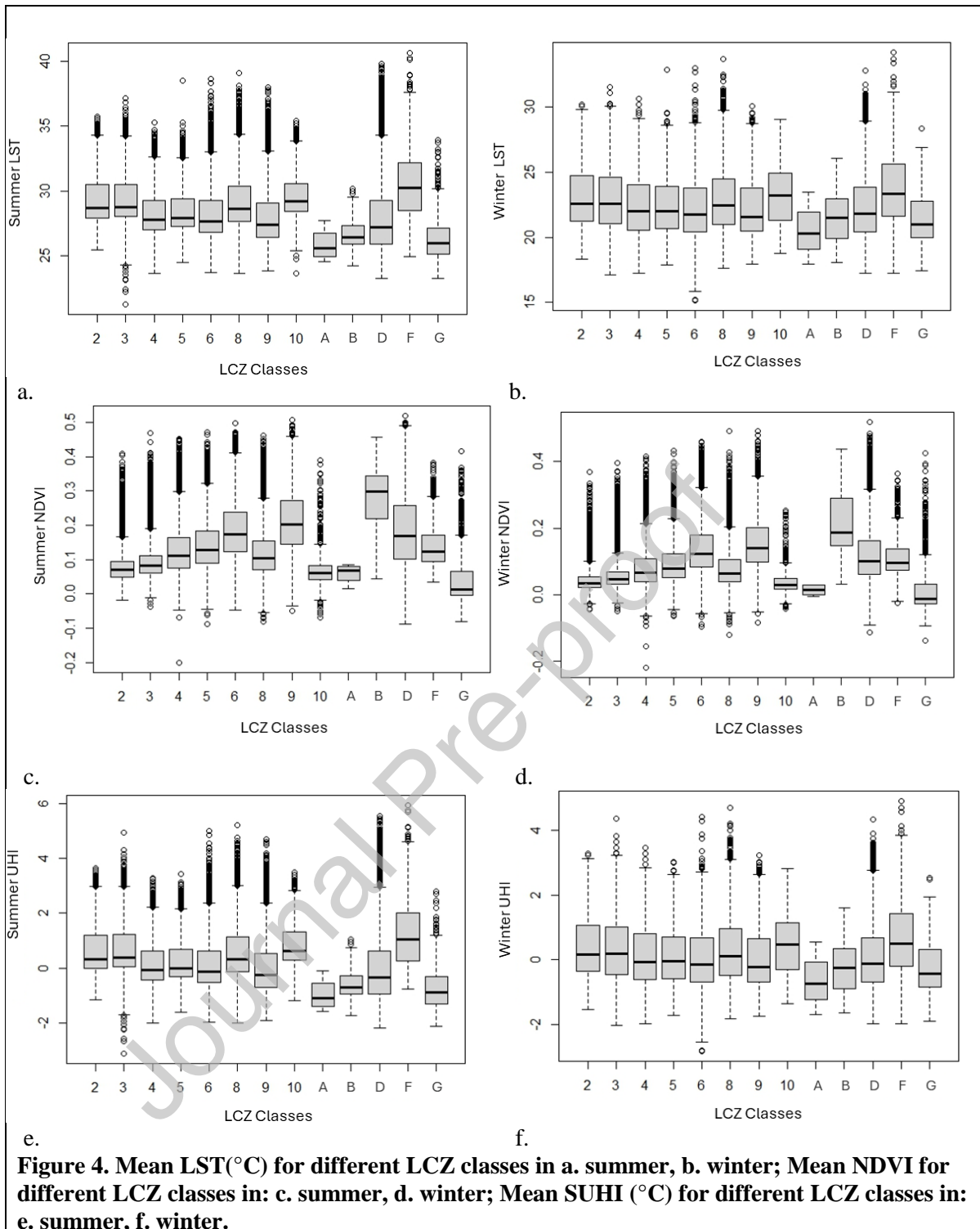




3.3. NDVI

NDVI is close to zero (0.1 and less) for more urbanised and vegetation-free areas or bare soil. Positive values of NDVI ranging from 0.10 to 0.50 indicate sparse vegetation such as shrubs and grasslands and values of 0.7 and above indicate dense green vegetation. The NDVI values for Dhaka are divided into five categories: no vegetation (mainly water bodies, negative values), poor vegetation (values between 0.10 and 0.30), sparse vegetation (values between 0.30 and 0.50), moderate to healthy vegetation (values between 0.50 and 0.70) and dense vegetation (values above 0.7). The Figure 3c and Figure 3d show the mean summer NDVI and mean winter NDVI, respectively. The summer NDVI is higher than the winter due to higher rainfall in summer compared to the dry, winter season in Dhaka. The NDVI ranges in Dhaka are between -0.01 to 0.49 with an average NDVI of 0.13 in summer and 0.08 in winter indicating severely critical vegetation conditions across the city. The variation of NDVI values throughout the year can be found in Appendix 3.

The Figure 4c and Figure 4d present NDVI across the LCZ classes during summer and winter respectively, demonstrating that NDVI values for the various LCZ classes are different. Since urban land specifically for the purpose of vegetation is generally limited, appropriate measures need to be taken according to the LCZ classes. The built-up LCZ classes LCZ-2, LCZ-3, LCZ-4, LCZ-5, and LCZ-6 have increasing median summer NDVI values of 0.07, 0.08, 0.11, 0.13, and 0.18 respectively as the building density reduces and amount of vegetation increases (see Table 2). LCZ-9 has a higher median summer NDVI (0.20) compared to LCZ-8 (0.10) and LCZ-10 (0.06) which have few or no trees. Landcover classes LCZ-B and LCZ-D has higher median summer NDVI of 0.30 and 0.17 respectively compared to LCZ-F (0.12) which has few or no trees. LCZ-A (Dense trees) is not considered because of the reason explained earlier. LCZ-G (Water) has a median summer NDVI of 0.01. Winter NDVI follows a similar pattern across the LCZ classes, except for the variation in magnitude.



3.4. SUHI

SUHI has a strong positive correlation with LST in both summer and winter with Spearman's rank correlation rho of 0.79 and 0.79, respectively. The Figure 3e and Figure 3f shows the SUHI impact during the summer and winter respectively in Dhaka with similar patterns. SUHI with values higher than 3.0° C is visible in the areas where most of the landfilling is occurring. Mostly located in the

east of the city these are the areas where the flood-flow-zones are being filled up for new housing projects. Higher SUHI are visible in the south of Uttara, located next to the International Airport. Among the built-up areas within the city, Tejgaon Industrial Area shows higher SUHI with its high-density, industrial, and commercial buildings. Abrar *et al.* [23] have also identified the Tejgaon Industrial Area as having the highest LST. Among other built-up areas, Hazaribagh Tannery and Chakbazar located in the southwest of the city, shows higher SUHI. In summer, SUHI intensity is higher in Kafrul, Mohammadpur, Badda, Tejgaon and Motijheel areas.

The Figure 4e and Figure 4f present the variation of SUHI for different LCZ classes in summer and winter, respectively. Like the LST patterns, more high-density and compact built-up areas such as LCZ-2 (Compact mid-rise) and LCZ-3 (Compact low-rise), industrial and commercial areas such as LCZ-8 (Large low-rise) and LCZ-10 (Heavy industry) have higher SUHI. All landcover classes have lower SUHI except LCZ-F (Bare soil or sand) where most of the landfilling is occurring. For the built-up LCZ classes, median winter SUHI is mostly lower compared to median summer SUHI. Landcover classes on the other hand have higher median winter SUHI than summer, except LCZ-F (Bare sand). Statistically significant and positive correlations (Spearman's rho) were found between population and SUHI for both summer (0.32) and winter (0.19) demonstrating that SUHI increases with the number of people per grid-cell (see Figure 5a and Figure 5b)). LCZ-F (Bare soil or sand) and LCZ-G (Water) were excluded from correlation analysis as these are not habitable areas. The magnitudes of the correlations were weak because of the missing population data for 5799 grid-cells covering 579900 m² area as mentioned earlier.

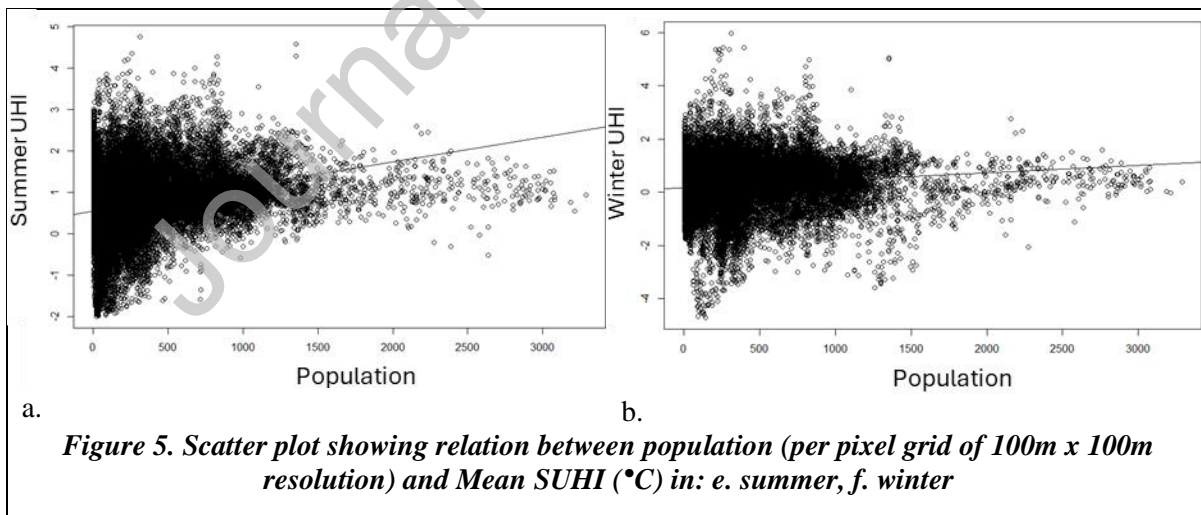


Table 2. Summary statistics for LST, NDVI, SUHI

LCZ	2	3	4	5	6	8	9	10	A	B	D	F	G
a. Summary statistics for LST													
Summer LST													
Min	25.5	24.3	23.7	24.5	23.7	23.7	23.8	25.4	24.6	24.2	23.3	24.9	23.3
First Quartile	27.9	28.1	27.0	27.3	26.8	27.7	26.4	28.4	24.9	25.9	25.9	28.5	25.1
Median	28.7	28.8	27.8	27.9	27.6	28.6	27.4	29.2	25.6	26.5	27.2	30.2	26.0
Third Quartile	30.5	30.5	29.3	29.4	29.3	30.4	29.1	30.6	26.8	27.4	29.3	32.2	27.2
Maximum	34.3	34.3	32.7	32.6	33.0	34.4	33.1	33.8	27.7	29.5	34.3	37.6	30.2
Winter LST													
Min	18.3	17.1	17.3	17.9	15.8	17.6	17.9	18.8	18.0	18.1	17.3	17.2	17.4
First Quartile	21.2	21.0	20.6	20.7	20.4	21.0	20.5	21.3	19.1	19.9	20.4	21.6	20.0
Median	22.6	22.6	22.0	22.0	21.8	22.4	21.6	23.2	20.3	21.5	21.8	23.4	21.0
Third Quartile	24.7	24.6	24.1	23.9	23.8	24.5	23.8	25.0	22.0	23.0	23.8	25.6	22.8
Maximum	29.8	30.1	29.1	28.6	28.8	29.8	28.7	29.1	23.5	26.1	28.9	31.2	26.9
b. Summary statistics for NDVI													
Summer NDVI													
Min	-0.02	-0.01	-0.05	-0.04	-0.05	-0.05	-0.03	-0.02	0.05	-0.09	0.03	-0.08	-0.02
First Quartile	0.05	0.06	0.08	0.09	0.12	0.07	0.15	0.04	0.22	0.10	0.10	0.00	0.05
Median	0.07	0.08	0.11	0.13	0.18	0.10	0.20	0.06	0.30	0.17	0.12	0.01	0.07
Third Quartile	0.10	0.11	0.16	0.18	0.24	0.16	0.27	0.08	0.35	0.26	0.17	0.07	0.10
Maximum	0.17	0.19	0.30	0.32	0.41	0.28	0.46	0.15	0.46	0.49	0.28	0.17	0.17
Winter NDVI													
Min	-0.03	-0.03	-0.06	-0.05	-0.06	-0.05	-0.05	-0.03	0.03	-0.09	-0.02	-0.09	-0.03
First Quartile	0.02	0.03	0.04	0.05	0.09	0.04	0.10	0.02	0.15	0.06	0.07	-0.03	0.02
Median	0.03	0.05	0.07	0.08	0.12	0.07	0.14	0.03	0.19	0.10	0.10	-0.01	0.03
Third Quartile	0.05	0.07	0.11	0.12	0.18	0.11	0.20	0.05	0.29	0.16	0.14	0.03	0.05
Maximum	0.10	0.13	0.21	0.23	0.32	0.20	0.36	0.10	0.44	0.32	0.23	0.12	0.10
c. Summary statistics for SUHI													
Summer SUHI													
Min	-1.2	-1.7	-2.0	-1.6	-2.0	-2.0	-1.9	-1.2	-1.7	-0.8	-1.2	-1.7	-2.0
First Quartile	0.0	0.1	-0.4	-0.3	-0.5	-0.1	-0.7	0.3	-1.0	0.3	0.0	0.1	-0.4
Median	0.3	0.1	-0.1	0.0	-0.1	0.3	-0.3	0.6	-0.7	1.1	0.3	0.1	-0.1
Third Quartile	1.2	1.2	0.6	0.7	0.6	1.1	0.5	1.3	-0.3	2.0	1.2	1.2	0.6
Maximum	3.0	3.0	2.2	2.2	2.4	3.0	2.4	2.8	0.7	4.6	3.0	3.0	2.2
Winter SUHI													
Min	-1.5	-2.0	-2.0	-1.7	-2.6	-1.8	-1.7	-1.4	-1.6	-2.0	-1.5	-2.0	-2.0
First Quartile	-0.4	-0.5	-0.6	-0.6	-0.7	-0.5	-0.7	-0.3	-0.9	-0.2	-0.4	-0.5	-0.6
Median	0.2	0.2	-0.1	0.0	-0.1	0.1	-0.2	0.5	-0.3	0.5	0.2	0.2	-0.1
Third Quartile	1.1	1.0	0.8	0.7	0.7	1.0	0.7	1.2	0.4	1.4	1.1	1.0	0.8
Maximum	3.1	3.2	2.9	2.7	2.7	3.1	2.7	2.8	1.6	3.9	3.1	3.2	2.9

3.5. MDC Analysis

To determine the statistical significance of the differences in estimated means, we applied the MDC for LST, as shown in Table 3, a. For summer, it shows differences between various LCZ classes are statistically significant (< 0.05) for most categories except between LCZ-2 and LCZ-8, LCZ-4 and LCZ-6, LCZ-9 and LCZ-D and LCZ-B and LCZ-G. However, in winter, the statistical significance of differences between various categories decreases. For instance, there is 'no difference' between compact built-up areas and LCZ-8 (Large low-rise) during this season. Notably, no statistically significant differences were observed between open built-up areas and LCZ-B and LCZ-D.

The crosstabulation presenting the MDC for NDVI (Table 3, b). shows the difference in their mean values is statistically significant (< 0.05) in most cases, except between LCZ-2 and LCZ-10 and between LCZ-5 and LCZ-F in summer. In winter, there is 'no difference' between LCZ-2 and LCZ-10, LCZ-4 and LCZ-8, and LCZ-D and LCZ-F.

The MDC for SUHI (Table 3, c) shows similar pattern to that of the MDC for LST. During summer, statistically significant differences among various LCZ categories are more pronounced, but during winter, these differences diminish significantly. Consequently, the distinctions between different LCZ-Categories become less evident with the changing seasons. This leads to the absence of statistical differences between the compact classes of LCZ-2 and LCZ-3, LCZ-2 and LCZ-8 and LCZ-3 and LCZ-8, as well as considering LCZ-4 and LCZ-5 as equivalent. Similarly, the open built-classes such as LCZ-4, 5 and 6 were similar as LCZ-B and LCZ-D.

Table 3. Minimum Detectable Change (MDC) for LST

a. MDC for LST																									
Summer LST													Winter LST												
	2	3	4	5	6	8	9	10	B	D	F	G	LCZ	2	3	4	5	6	8	9	10	B	D	F	G
2		1	1	1	1	0	1	1	1	1	1	1	2		0	1	1	1	0	1	1	1	1	1	1
3			1	1	1	1	1	1	1	1	1	1	3			1	1	1	0	1	1	1	1	1	1
4				1	0	1	1	1	1	1	1	1	4				0	1	1	1	1	0	0	1	1
5					1	1	1	1	1	1	1	1	5					1	1	1	1	0	0	1	1
6						1	1	1	1	1	1	1	6						1	0	1	0	1	1	1
8							1	1	1	1	1	1	8							1	1	1	1	1	1
9								1	1	0	1	1	9								1	0	1	1	1
10									1	1	1	1	10									1	1	1	1
12										1	1	0	12										0	1	0
14											1	1	14											1	1
16												1	16												1
b. MDC for NDVI																									
Summer NDVI													Winter NDVI												
	2	3	4	5	6	8	9	10	B	D	F	G	LCZ	2	3	4	5	6	8	9	10	B	D	F	G
2		1	1	1	1	1	1	0	1	1	1	1	2		1	1	1	1	1	1	0	1	1	1	1
3			1	1	1	1	1	1	1	1	1	1	3			1	1	1	1	1	1	1	1	1	1
4				1	1	1	1	1	1	1	1	1	4				1	1	0	1	1	1	1	1	1
5					1	1	1	1	1	1	0	1	5					1	1	1	1	1	1	1	1
6						1	1	1	1	1	1	1	6						1	1	1	1	1	1	1
8							1	1	1	1	1	1	8							1	1	1	1	1	1
9								1	1	1	1	1	9								1	1	1	1	1
10									1	1	1	1	10									1	1	1	1
12										1	1	1	12										1	1	1
14											1	1	14											0	1
16												1	16												1
c. MDC for SUHI																									
Summer SUHI													Winter SUHI												
	2	3	4	5	6	8	9	10	B	D	F	G	LCZ	2	3	4	5	6	8	9	10	B	D	F	G
2		1	1	1	1	0	1	1	1	1	1	1	2		0	1	1	1	0	1	1	1	1	1	1
3			1	1	1	1	1	1	1	1	1	1	3			1	1	1	0	1	1	1	1	1	1
4				1	0	1	1	1	1	1	1	1	4				0	1	1	1	1	0	0	1	1
5					1	1	1	1	1	1	1	1	5					1	1	1	1	0	0	1	1
6						1	1	1	1	1	1	1	6						1	0	1	0	1	1	1
8							1	1	1	1	1	1	8							1	1	1	1	1	1
9								1	1	0	1	1	9								1	0	1	1	1
10									1	1	1	1	10									1	1	1	1
12										1	1	0	12										0	1	0
14											1	1	14											1	1
16												1	16												1

4. Discussion

4.1. LST characteristics in LCZ

In this study, significant differences in LST were observed between various LCZ categories within Dhaka. Most of the city's built environment falls into LCZ-2 (Compact mid-rise), LCZ-3 (Compact low-rise), LCZ-5 (Open mid-rise) and LCZ-6 (Open low-rise). We found that the mean LST

difference between the compact built-classes (LCZ-2, LCZ-3, LCZ-8, LCZ-10) and open built-classes (LCZ-4-LCZ-6, LCZ-9) is 1.2°C in summer and 0.8°C in winter. Furthermore, natural landcover classes (LCZ-A, LCZ-B, LCZ-D) are 2.4°C and 1.3°C cooler in summer than compact built-classes and open built-classes, respectively.

These findings are consistent with previous studies from other urban settings. For instance, research from Sendai, a typical Japanese metropolitan city, showed that LSTs in compact residential areas were higher than those in commercial areas at the city-centre [63]. Similarly, in Kumasi city, Ghana [64] a rise of 1.2°C in average surface temperature was linked to urbanisation. In Berlin, Germany, a study observed an average temperature difference of about 1.0°C (K) during summer nights between dense-trees (LCZ-A) and LCZ-6 (Open low-rise) areas [65]. These variations underline the broader implications for urban climate, especially as heatwaves become more frequent. Consequently, incorporating open built-classes into the planning of new or existing urban areas can have a substantial impact on reducing LST and thereby, ultimately enhancing the local microclimate.

In this study, LSTs in the large low-rise buildings (LCZ-8) and heavy industrial buildings (LCZ-10) categories frequently surpass those observed in other compact built-classes (LCZ-2, 3, and 4). Numerous studies have described the higher LSTs of industrial areas during daytime [66]–[68]. This trend is attributed to the prevalence of impervious surfaces and extensive roof areas with low albedo, aligning with findings from earlier research studies [9], [69]. These areas require additional vegetation for increased shading and reduced albedo on roof surfaces to mitigate solar radiation in summer. A more detailed analysis, incorporating factors such as vegetation type, density, surface fraction, and thermal properties of pervious surfaces, is essential for developing effective strategies to reduce LST in LCZ-8 and LCZ-10 [70].

4.2. NDVI characteristics in LCZ

Regarding NDVI in Dhaka, even the open built-classes display a significant lack of vegetation with a mean NDVI of 0.15 in summer. None of the areas in the city exhibit moderate to healthy vegetation, indicating a significant lack of permeable surfaces and an excessive presence of paved or impermeable surfaces. This contributes to the escalating extreme heat conditions within the city. Moreover, it severely impacts the city's sustainable drainage, albeit almost non-existent, leading to severe damage during Monsoon rains and causing floods. Although LCZ-9 and LCZ-D show higher levels of NDVI compared to other areas with a median NDVI of 0.20 and 0.17 in summer, respectively, they still fall short of having healthy vegetation levels. Currently, the north-east and south-east regions of the city display some sparse vegetation, with NDVI values ranging between 0.3 and 0.5 in summer. Nevertheless, if the current growth trend persists, these areas are at risk of being encroached upon by buildings, leading to further reduction in vegetation and agricultural land.

Undoubtedly, this will exacerbate flood conditions during the Monsoon season and intensify extreme heat situations in the summer, rendering the living conditions completely unviable.

Previous studies have demonstrated that vegetation has a cooling effect on urban areas [71]–[73] that lies between 1–3°C (K) [71] and thus increasing vegetation can mitigate the SUHI. The magnitude and nature of this relation can be variable depending on the vegetation and built environment pattern. Warming has been noticed in areas with scarce vegetation and/or bare soils [74], [75].

Several studies have examined NDVI in association with their LCZ classes. For example, a study conducted by [76] in three Chinese metropolises, Wuhan, Nanjing, and Shanghai found that NDVI exhibited a more significant mitigating effect on Heat Risk Index (HRI) in LCZ-1, LCZ-2, LCZ-4 and LCZ-5. To alleviate heat risk, their recommendations included updating compact LCZ types to open LCZ types, avoiding the configuration of LCZ-1 and LCZ-2, prioritising NDVI enhancement in existing LCZ-1, LCZ-2, LCZ-4 and LCZ-5 areas, increasing greenery by upgrading mono-structures to composite structures with trees, shrubs, and grasses, and implementing greening of facades. Other studies, such as [77] in China, have reported that NDVI has a remarkable cooling effect on the SUHI for the vast majority of the year. They also found that NDVI performed best in cooling within the LCZ-F, especially in summer and spring.

It is important to understand the impact of vegetation on LST to identify the areas which are vulnerable to heat and how these can be rectified through vegetation. Numerous studies have established the cooling effect of vegetation cover on surface temperatures, effectively mitigating SUHI phenomena [78]. The cooling effect of vegetation and green spaces works through evapotranspiration, photosynthesis, blocking of shortwave radiation and shadow casting and trapping of longwave radiation [79]. Therefore, green spaces play a significant role in moderating thermal environments, especially during the hot period [80]. In this study mean summer and winter LSTs were tested against associated NDVIs using linear regressions. As expected, negative associations were found between LST and NDVI with Spearman's rank correlation rho of 0.424 in summer and 0.174 in winter, also reported in other studies [77].

4.3. SUHI characteristics in LCZ

In this study, the differences in maximum SUHI between the compact (LCZ-2, LCZ-3, LCZ-8, LCZ-10) and open (LCZ-4, LCZ-5, LCZ-6, LCZ-9) built-classes is 0.7°C in summer and 0.4°C in winter (Table 2). Among the built-classes in summer, LCZ-2, LCZ-3 and LCZ-8 exhibits the highest maximum SUHI (3.0°C), while LCZ-4 and LCZ-5 has the lowest maximum SUHI (2.2°C) and in winter, LCZ-3 shows the highest maximum SUHI (3.2°C) and LCZ-5, LCZ-6 and LCZ-9 shows the lowest (2.7°C) winter (Table 2). In both summer and winter, LCZ-F is found to have the maximum SUHI of 4.6°C and 3.9°C, respectively (Table 2). In agreement with these results, a recent study has revealed that urban expansion and dense settlements have led to a nearly 3.0°C increase in average

surface temperature in certain areas of Dhaka city compared to its boundary [81]. A similar study in Delhi [82] show an SUHI intensity of 3.5°C, as the difference between LCZ-3 (compact low-rise) and LCZ-D (low plants), which occurs in summer.

This study findings also suggest that compact built-classes along with large low-rise buildings (LCZ-8) and heavy industrial buildings (LCZ-10) have a similar impact on the local microclimate as the compact LCZ classes. Their morphological configuration restricts airflow through the buildings and surrounding spaces, while their large masses absorb high levels of solar radiation, leading to higher LSTs and SUHI. LCZ-10 areas also generate a significant amount of heat during the industrial processes which is released into the surrounding environment [9], resulting in higher SUHI.

LCZ system has been widely applied in studies focusing on SUHI [83]. Studies by [84] evaluated LST characteristics across 18 LCZs in Beijing, revealing that the warmest zones are compact and mid to low-rise built-up areas (LCZ-2, LCZ-3, LCZ-7, LCZ-8) while the coolest zones are water and vegetated types (LCZ-A, LCZ-B, LCZ-D, LCZ-G) with SUHI events being most frequent during summertime and daytime conditions. Additionally, LCZ-9 and LCZ-A, LCZ-B, LCZ-D, and LCZ-G exhibited a seasonal pattern with smaller Annual Temperature Ranges (ATRs) attributed to factors such as leaf abscission, crop harvesting, and irrigation schedules, whereas high-rise built-up zones (LCZ-1 and LCZ-4) experienced higher ATRs due to seasonal variations in solar radiation through shade effects and convective heat dissipation capabilities. Recent studies [85] have analysed the correlation between SUHI intensity and LCZ classes in Budapest, reinforcing that as building density decreases, SUHI intensities also decrease. They found the highest intensities in the city centre, while vegetated landcover LCZ classes show the lowest SUHI intensities, sometimes with negative values indicating cooling.

4.4. LCZ Application for Dhaka

In this study, all open built-classes show positive impacts on microclimate with LCZ-4 (Open high-rise) and LCZ-6 performing slightly better than LCZ-5 (Open mid-rise) while comparing their median LSTs and SUHIs. However, despite falling into the category of open built-classes, LCZ-6 (Open low-rise) may not be the optimal choice for Dhaka, given its constantly growing population. In a similar study in Delhi, [82] have suggested that in order to minimise the UHI effect, further urban expansion in the Delhi region should be restricted to LCZ-5 (open mid-rise) and LCZ-6 (open low-rise). Considering the high-density context of Dhaka, a more suitable approach may involve replacing LCZ-3 (Compact low-rise) with a combination of LCZ-4 (Open high-rise) and LCZ-5 (Open mid-rise). This adjustment is likely to yield better results and contribute positively to the city's climate management. The inclusion of LCZ-4 (Open high-rise) can be further justified by recent research [86] [86] which indicates that increasing building density with taller structures leads to a slower escalation in AUHI intensity. This impact is particularly pronounced with larger street

canyon aspect ratios. Additionally, although LCZ-9 demonstrates better performance than the open built-classes in this study, it may not be suitable for accommodating Dhaka's large population. In contrast, the cooling effects observed in LCZ-4 (Open high-rise) areas, attributed to buildings shading and higher vegetation density, make it a more viable option, as also supported by findings in previous studies [70], [87], [88].

4.5. Effectiveness of LCZ classes

The results of this study also highlight the effectiveness of the LCZ classes in identifying the microclimatic diversity as demonstrated by MDC analysis. Notably, statistically significant differences were observed in NDVI values among various LCZ categories. For the LST and SUHI, distinct variations were evident between the LCZ categories during the summer. However, these distinctions dwindled during winter, particularly between the open built-classes (LCZ-4, LCZ-5, and LCZ-6) and green landcover classes (LCZ-B and LCZ-D). While LCZ may not provide complete effectiveness in distinguishing variations in urban morphology, it remains suitable for distinguishing between broader categories such as compact and open built-classes, as well as green and bare soil landcover classes. Therefore, it proves to be a valuable tool for guiding urban planning and design decisions aimed at enhancing microclimates and mitigating climate impacts in high-density cities.

5. Conclusion

Recent studies [89] highlight a significant gap in documenting SUHI effects in tropical regions compared to temperate climates, underscoring a disconnect between scientific research and its practical application in urban planning. This study addresses this gap by analysing the relationship between urban morphology, LST, NDVI, and SUHI in Dhaka using a LCZ map. This approach provides globally consistent data essential for supporting climate-modelling and developing evidence-based, climate-sensitive urban planning policies. Particularly, the spatial distributions of LST, NDVI and SUHI as per the LCZ classes are critical for understanding the urban thermal environment in a tropical, megacity context. Key findings indicate higher LSTs in built-up areas, particularly LCZ-8 (Large low-rise) and LCZ-5 (Open mid-rise) during summer and LCZ-3 (Compact low-rise) and LCZ-5 in winter. Open built-classes were cooler than compact ones, suggesting urban planning strategies to mitigate heat could include integrating more open high-rise (LCZ-4) and mid-rise (LCZ-5) structures instead of compact low-rise areas (LCZ-3).

Additionally, vegetation cover was found to significantly lower surface temperatures, indicating the importance of maintaining green spaces to counteract increasing LST and SUHI. The negative correlation observed between LST and NDVI suggests that replacing agricultural land in flood-flow

zones with built-up areas will exacerbate LST and SUHI increases. Consequently, urban planning policies must prioritise ecological conservation to address this challenge.

In terms of SUHI impact, the maximum summer values in these areas reach 3.0°C, with peaks up to 3.6°C and 4.9°C. This indicates that residents in high-density areas are particularly vulnerable to SUHI effects. While SUHI can adversely impact any climate or city, cities in developing countries are especially susceptible due to limited resources and reduced adaptive capacity, making effective urban planning and resource management crucial.

Given Dhaka's dense population and continuous urban transformations, these insights are crucial for developing evidence-based, climate-sensitive urban planning policies. Strategies should include enhancing urban greenery, using pervious and low-albedo materials, and reducing high-density development to effectively manage heat in urban settings.

In conclusion, this study establishes a robust framework for applying LCZ classification in tropical megacities. It provides crucial data for urban planners, demonstrating the advantages of using LCZ classification over traditional land use and land cover (LULC) methods to better understand urban thermal dynamics, thereby enhancing the planning and management of urban climates.

Declaration of Competing Interest: The authors declare that they have no known competing financial interests or personal relationships that could have appeared to influence the work reported in this paper.

Data availability statement: The datasets used and/or analysed during the study are publicly available from the United States Geological Survey EarthExplorer from this link:
<https://earthexplorer.usgs.gov/>.

Acknowledgement

The time and resources dedicated for this work is funded by the Fung Global Fellowship Program at Princeton University. The author is grateful to Tsering Wangyal Shawa, Head of Princeton University Map and Geospatial Information Center for providing necessary GIS training and support.

Funding

This work is funded by the Fung Global Fellowship Program at Princeton University.

CRedit authorship contribution statement

Tania Sharmin: Conceptualization; Data curation; Formal analysis; Funding acquisition; Investigation; Methodology; Project administration; Resources; Software; Validation; Visualization; Roles/Writing - original draft; Writing - review & editing.

Adrian Chappell: Validation; Writing - review & editing.

Reference

- [1] D. Hidalgo García and J. Arco Díaz, “Modeling of the Urban Heat Island on local climatic zones of a city using Sentinel 3 images: Urban determining factors,” *Urban Clim.*, vol. 37, no. September 2020, 2021, doi: 10.1016/j.uclim.2021.100840.
- [2] World Economic Forum, “The Global Risks Report 2018: The risks of rapid urbanization in developing countries,” 2018. [Online]. Available: <https://www.zurich.com/en/knowledge/topics/global-risks/the-risks-of-rapid-urbanization-in-developing-countries>
- [3] U.S. Environmental Protection Agency, “Urban Heat Island Basics. Reducing Urban Heat Islands : Compendium of Strategies,” 2008. [Online]. Available: <https://www.epa.gov/heat-islands/heat-island-compendium>
- [4] D. Khamchiangta and S. Dhakal, “Physical and non-physical factors driving urban heat island: Case of Bangkok Metropolitan Administration, Thailand,” *J. Environ. Manage.*, vol. 248, no. July 2020, 2019, doi: 10.1016/j.jenvman.2019.109285.
- [5] C. Tuholske, K. Caylor, C. Funk, A. Verdin, S. Sweeney, and K. Grace, “Global urban population exposure to extreme heat,” pp. 1–9, 2021, doi: 10.1073/pnas.2024792118.
- [6] X. Zhou *et al.*, “Exploring the impacts of heat release of vehicles on urban heat mitigation in Sendai , Japan using WRF model integrated with urban LCZ,” *Sustain. Cities Soc.*, vol. 82, no. January, p. 103922, 2022, doi: 10.1016/j.scs.2022.103922.
- [7] S. Funk, B. Rao, T. Alcayna, I. Fletcher, and R. Gibb, “Review Climate-sensitive disease outbreaks in the aftermath of extreme climatic events : A scoping review,” 2022, doi: 10.1016/j.oneear.2022.03.011.
- [8] J. Tan, D. Yu, Q. Li, X. Tan, and W. Zhou, “Spatial relationship between land-use/land-cover change and land surface temperature in the Dongting Lake area, China,” *Sci. Rep.*, vol. 10, no. 1, pp. 1–9, 2020, doi: 10.1038/s41598-020-66168-6.
- [9] E. Matsaba, E. Fakhazadehshirazi, A. Ochieng, J. Bosco, J. Mwibanda, and S. Sodoudi, “Urban Climate Inter-local climate zone differentiation of land surface temperatures for Management of Urban Heat in Nairobi City , Kenya,” *Urban Clim.*, vol. 31, no. September 2019, p. 100540, 2020, doi: 10.1016/j.uclim.2019.100540.

- [10] J. Song, W. Chen, J. Zhang, K. Huang, B. Hou, and A. V. Prishchepov, "Effects of building density on land surface temperature in China: Spatial patterns and determinants," *Landsc. Urban Plan.*, vol. 198, no. September 2019, p. 103794, 2020, doi: 10.1016/j.landurbplan.2020.103794.
- [11] I. Hough, A. C. Just, B. Zhou, M. Dorman, J. Lepeule, and I. Kloog, "A multi-resolution air temperature model for France from MODIS and Landsat thermal data," *Environ. Res.*, vol. 183, no. January, p. 109244, 2020, doi: 10.1016/j.envres.2020.109244.
- [12] I. D. Stewart and G. Mills, "The Urban Heat Island: A Guidebook," *Urban Heat Isl.*, pp. 1–171, 2021, doi: 10.1016/B978-0-12-815017-7.09997-5.
- [13] A. Chappell, C. Strong, G. McTainsh, and J. Leys, "Detecting induced in situ erodibility of a dust-producing playa in Australia using a bi-directional soil spectral reflectance model," *Remote Sens. Environ.*, vol. 106, no. 4, pp. 508–524, 2007, doi: 10.1016/j.rse.2006.09.009.
- [14] T. He *et al.*, "Evaluating land surface albedo estimation from Landsat MSS, TM, ETM+, and OLI data based on the unified direct estimation approach," *Remote Sens. Environ.*, vol. 204, no. October 2017, pp. 181–196, 2018, doi: 10.1016/j.rse.2017.10.031.
- [15] L. Hu and N. A. Brunsell, "A new perspective to assess the urban heat island through remotely sensed atmospheric profiles," *Remote Sens. Environ.*, vol. 158, pp. 393–406, 2015, doi: 10.1016/j.rse.2014.10.022.
- [16] H. Shen, L. Huang, L. Zhang, P. Wu, and C. Zeng, "Long-term and fine-scale satellite monitoring of the urban heat island effect by the fusion of multi-temporal and multi-sensor remote sensed data: A 26-year case study of the city of Wuhan in China," *Remote Sens. Environ.*, vol. 172, pp. 109–125, 2016, doi: 10.1016/j.rse.2015.11.005.
- [17] I. D. Stewart and T. R. Oke, "Local climate zones for urban temperature studies," *Bull. Am. Meteorol. Soc.*, vol. 93, no. 12, pp. 1879–1900, 2012, doi: 10.1175/BAMS-D-11-00019.1.
- [18] The World Bank, "Population in largest city - Bangladesh." [Online]. Available: <https://data.worldbank.org/indicator/EN.URB.LCTY?end=2021&locations=BD&start=2021&view=bar>
- [19] I. Ahmed, "Factors in building resilience in urban slums of Dhaka, Bangladesh," *Procedia Econ. Financ.*, vol. 18, no. September, pp. 745–753, 2014, doi: 10.1016/s2212-5671(14)00998-8.
- [20] S. M. Satter *et al.*, "Transmission of SARS-CoV-2 in the Population Living in High-and Low-Density Gradient Areas in Dhaka, Bangladesh," *Trop. Med. Infect. Dis.*, vol. 7, no. 4, pp. 1–14, 2022, doi: 10.3390/tropicalmed7040053.
- [21] S. Hossain, "The production of space in the negotiation of water and electricity supply in a bosti of Dhaka," *Habitat Int.*, vol. 36, no. 1, pp. 68–77, 2012, doi: 10.1016/j.habitatint.2011.05.007.
- [22] A. Dewan, G. Kiselev, D. Botje, G. I. Mahmud, M. H. Bhuian, and Q. K. Hassan, "Surface

- urban heat island intensity in five major cities of Bangladesh: Patterns, drivers and trends,” *Sustain. Cities Soc.*, vol. 71, no. April, p. 102926, 2021, doi: 10.1016/j.scs.2021.102926.
- [23] R. Abrar *et al.*, “Assessing the Spatial Mapping of Heat Vulnerability under Urban Heat Island (UHI) Effect in the Dhaka Metropolitan Area,” *Sustain.*, vol. 14, no. 9, 2022, doi: 10.3390/su14094945.
- [24] RAJUK, “Detailed Area Plan (DAP) - Development Plan for Dhaka City.” [Online]. Available: <http://www.rajuk.gov.bd/site/page/68c8d4af-f493-43de-a54c-b0dc83d56bff/>
- [25] M. J. Alam and M. M. Ahmad, “Analysing the lacunae in planning and implementation: Spatial development of dhaka city and its impacts upon the built environment,” *Int. J. Urban Sustain. Dev.*, vol. 2, no. 1–2, pp. 85–106, 2010, doi: 10.1080/19463138.2010.512809.
- [26] M. J. Alam, ““the organized encroachment of land developers’ - Effects on urban flood management in Greater Dhaka, Bangladesh,” *Sustain. Cities Soc.*, vol. 10, pp. 49–58, 2014, doi: 10.1016/j.scs.2013.05.006.
- [27] K. H. Razimul Karim, “Trends of Permanent Wetland Change in Detailed Area Plan of Dhaka,” *Am. J. Water Resour.*, vol. 2, no. 5, pp. 106–109, 2014, doi: 10.12691/ajwr-2-5-1.
- [28] F. Ahmed, E. Moors, M. S. A. Khan, J. Warner, and C. Terwisscha van Scheltinga, “Tipping points in adaptation to urban flooding under climate change and urban growth: The case of the Dhaka megacity,” *Land use policy*, vol. 79, no. May, pp. 496–506, 2018, doi: 10.1016/j.landusepol.2018.05.051.
- [29] M. Alam and G. M. D. Rabbani, “Vulnerabilities and responses to climate change for Dhaka,” *Environ. Urban.*, vol. 19, no. 1, pp. 81–97, 2007, doi: 10.1177/0956247807076911.
- [30] Japan International Cooperation Agency (JICA), “Study on stormwater drainage system improvement project in Dhaka city,” 1987.
- [31] T. Sharmin, K. Steemers, and A. Matzarakis, “Analysis of microclimatic diversity and outdoor thermal comfort perceptions in the tropical megacity Dhaka, Bangladesh,” *Build. Environ.*, vol. 94, pp. 734–750, Dec. 2015, doi: 10.1016/j.buildenv.2015.10.007.
- [32] M. Demuzere, J. Kittner, and B. Bechtel, “LCZ Generator: A Web Application to Create Local Climate Zone Maps,” *Front. Environ. Sci.*, vol. 9, no. April, 2021, doi: 10.3389/fenvs.2021.637455.
- [33] M. Vaidya, R. Keskar, and R. Kotharkar, “Classifying heterogeneous urban form into local climate zones using supervised learning and greedy clustering incorporating Landsat dataset,” *Urban Clim.*, vol. 53, no. November 2023, p. 101770, 2024, doi: 10.1016/j.uclim.2023.101770.
- [34] Y. Xu, C. Ren, M. Cai, N. Y. Y. Edward, and T. Wu, “Classification of Local Climate Zones Using ASTER and Landsat Data for High-Density Cities,” *IEEE J. Sel. Top. Appl. Earth Obs. Remote Sens.*, vol. 10, no. 7, pp. 3397–3405, 2017, doi: 10.1109/JSTARS.2017.2683484.
- [35] G. Xu, X. Zhu, N. Tapper, and B. Bechtel, “Urban climate zone classification using

- convolutional neural network and ground-level images,” *Prog. Phys. Geogr.*, vol. 43, no. 3, pp. 410–424, 2019, doi: 10.1177/0309133319837711.
- [36] C. Ru *et al.*, “Land Surface Temperature Retrieval from Landsat 8 Thermal Infrared Data over Urban Areas Considering Geometry Effect: Method and Application,” *IEEE Trans. Geosci. Remote Sens.*, vol. 60, pp. 1–16, 2022, doi: 10.1109/TGRS.2021.3088482.
- [37] M. Lemus-Canovas, J. Martin-Vide, M. C. Moreno-Garcia, and J. A. Lopez-Bustins, “Estimating Barcelona’s metropolitan daytime hot and cold poles using Landsat-8 Land Surface Temperature,” *Sci. Total Environ.*, vol. 699, p. 134307, 2020, doi: 10.1016/j.scitotenv.2019.134307.
- [38] C. B. Pande *et al.*, “Predictive modeling of land surface temperature (LST) based on Landsat-8 satellite data and machine learning models for sustainable development,” *J. Clean. Prod.*, vol. 444, no. February, p. 141035, 2024, doi: 10.1016/j.jclepro.2024.141035.
- [39] D. Kumar, A. Soni, and M. Kumar, “Retrieval of Land Surface Temperature from Landsat-8 Thermal Infrared Sensor Data,” *J. Human, Earth, Futur.*, vol. 3, no. 2, pp. 159–168, 2022, doi: 10.28991/HEF-2022-03-02-02.
- [40] S. Guha, H. Govil, A. Dey, and N. Gill, “Analytical study of land surface temperature with NDVI and NDBI using Landsat 8 OLI and TIRS data in Florence and Naples city, Italy,” *Eur. J. Remote Sens.*, vol. 51, no. 1, pp. 667–678, 2018, doi: 10.1080/22797254.2018.1474494.
- [41] P. S. Kafer, S. B. A. Rolim, M. L. Iglesias, N. S. Da Rocha, and L. R. Diaz, “Land surface temperature retrieval by landsat 8 thermal band: Applications of laboratory and field measurements,” *IEEE J. Sel. Top. Appl. Earth Obs. Remote Sens.*, vol. 12, no. 7, pp. 2332–2341, 2019, doi: 10.1109/JSTARS.2019.2913822.
- [42] S. A. Ali, F. Parvin, and A. Ahmad, “Retrieval of Land Surface Temperature from Landsat 8 OLI and TIRS: A Comparative Analysis Between Radiative Transfer Equation-Based Method and Split-Window Algorithm,” *Remote Sens. Earth Syst. Sci.*, vol. 6, no. 1–2, pp. 1–21, 2023, doi: 10.1007/s41976-022-00079-0.
- [43] B. J. He, Z. Q. Zhao, L. Du Shen, H. B. Wang, and L. G. Li, “An approach to examining performances of cool/hot sources in mitigating/enhancing land surface temperature under different temperature backgrounds based on landsat 8 image,” *Sustain. Cities Soc.*, vol. 44, no. March 2018, pp. 416–427, 2019, doi: 10.1016/j.scs.2018.10.049.
- [44] Q. Weng, D. Lu, and J. Schubring, “Estimation of land surface temperature-vegetation abundance relationship for urban heat island studies,” *Remote Sens. Environ.*, vol. 89, no. 4, pp. 467–483, 2004, doi: 10.1016/j.rse.2003.11.005.
- [45] W. C. Snyder, Z. Wan, Y. Zhang, and Y. Z. Feng, “Classification-based emissivity for land surface temperature measurement from space,” *Int. J. Remote Sens.*, vol. 19, no. 14, pp. 2753–2774, 1998, doi: 10.1080/014311698214497.
- [46] L. Congedo, “Semi-Automatic Classification Plugin Documentation 5.0.0.1 Luca Congedo,”

- 2016, [Online]. Available:
<https://media.readthedocs.org/pdf/semiautomaticclassificationmanual-v5-fa/latest/semiautomaticclassificationmanual-v5-fa.pdf>
- [47] J. Geletič, M. Lehnert, and P. Dobrovolný, “Land surface temperature differences within local climate zones, Based on two central European cities,” *Remote Sens.*, vol. 8, no. 10, pp. 1–18, 2016, doi: 10.3390/rs8100788.
- [48] M. Cai, C. Ren, Y. Xu, K. K. L. Lau, and R. Wang, “Investigating the relationship between local climate zone and land surface temperature using an improved WUDAPT methodology – A case study of Yangtze River Delta, China,” *Urban Clim.*, vol. 24, pp. 485–502, 2018, doi: 10.1016/j.uclim.2017.05.010.
- [49] GISGeography, “What is NDVI (Normalized Difference Vegetation Index)?” [Online]. Available: <https://gisgeography.com/ndvi-normalized-difference-vegetation-index/>
- [50] Y. Hu, M. Hou, G. Jia, C. Zhao, X. Zhen, and Y. Xu, “Comparison of surface and canopy urban heat islands within megacities of eastern China,” *ISPRS J. Photogramm. Remote Sens.*, vol. 156, no. August, pp. 160–168, 2019, doi: 10.1016/j.isprsjprs.2019.08.012.
- [51] T. R. OKE, “CITY SIZE AND THE URBAN HEAT ISLAND,” *Atmos. Environ. Pergamon Press*, vol. 7, pp. 769–779, 1973, doi: 10.1126/science.147.3660.920-a.
- [52] S. W. Kim and R. D. Brown, “Urban heat island (UHI) intensity and magnitude estimations: A systematic literature review,” *Sci. Total Environ.*, vol. 779, p. 146389, 2021, doi: 10.1016/j.scitotenv.2021.146389.
- [53] B. Han, Z. Luo, Y. Liu, T. Zhang, and L. Yang, “Using Local Climate Zones to investigate Spatio-temporal evolution of thermal environment at the urban regional level: A case study in Xi’an, China,” *Sustain. Cities Soc.*, vol. 76, no. July 2021, p. 103495, 2022, doi: 10.1016/j.scs.2021.103495.
- [54] Z. Shi, J. Yang, Y. Zhang, X. Xiao, and J. C. Xia, “Urban ventilation corridors and spatiotemporal divergence patterns of urban heat island intensity: a local climate zone perspective,” *Environ. Sci. Pollut. Res.*, vol. 29, no. 49, pp. 74394–74406, 2022, doi: 10.1007/s11356-022-21037-9.
- [55] M. N. Rahman *et al.*, “Impact of Urbanization on Urban Heat Island Intensity in Major Districts of Bangladesh Using Remote Sensing and Geo-Spatial Tools,” *Climate*, vol. 10, no. 1, 2022, doi: 10.3390/cli10010003.
- [56] N. P. Webb *et al.*, “Reducing Sampling Uncertainty in Aeolian Research to Improve Change Detection,” *J. Geophys. Res. Earth Surf.*, vol. 124, no. 6, pp. 1366–1377, 2019, doi: 10.1029/2019JF005042.
- [57] P. E. Muckelt *et al.*, “Protocol and reference values for minimal detectable change of MyotonPRO and ultrasound imaging measurements of muscle and subcutaneous tissue,” *Sci. Rep.*, vol. 12, no. 1, pp. 1–11, 2022, doi: 10.1038/s41598-022-17507-2.

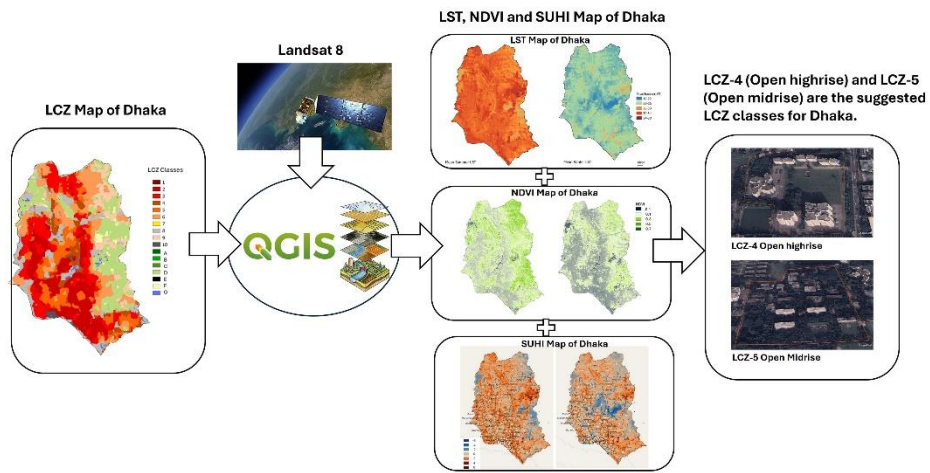
- [58] UNICEF, “UNICEF Bangladesh - For every child, freedom,” 2022. [Online]. Available: <https://www.unicef.org/bangladesh/en>
- [59] Bangladesh Bureau of Statistics, “Socio-Economic and Demographic Survey of Slum Dwellers of Dhaka SMA 1987,” 1987. [Online]. Available: <http://data.bbs.gov.bd/index.php/catalog/40/study-description>
- [60] L. Mentaschi *et al.*, “Global long-term mapping of surface temperature shows intensified intra-city urban heat island extremes,” *Glob. Environ. Chang.*, vol. 72, no. April 2021, 2022, doi: 10.1016/j.gloenvcha.2021.102441.
- [61] J. A. Voogt and T. R. Oke, “Thermal remote sensing of urban climates,” *Remote Sens. Environ.*, vol. 86, no. 3, pp. 370–384, 2003, doi: 10.1016/S0034-4257(03)00079-8.
- [62] L. S. Ferreira and D. H. S. Duarte, “Exploring the relationship between urban form, land surface temperature and vegetation indices in a subtropical megacity,” *Urban Clim.*, vol. 27, no. November 2018, pp. 105–123, 2019, doi: 10.1016/j.uclim.2018.11.002.
- [63] X. Zhou, T. Okaze, C. Ren, M. Cai, Y. Ishida, and H. Watanabe, “Evaluation of urban heat islands using local climate zones and the influence of sea-land breeze,” *Sustain. Cities Soc.*, vol. 55, no. October 2019, p. 102060, 2020, doi: 10.1016/j.scs.2020.102060.
- [64] C. Mensah *et al.*, “Impact of urban land cover change on the garden city status and land surface temperature of Kumasi Impact of urban land cover change on the garden city status and land surface temperature of Kumasi,” *Cogent Environ. Sci.*, vol. 6, no. 1, 2020, doi: 10.1080/23311843.2020.1787738.
- [65] D. Fenner, F. Meier, D. Scherer, and A. Polze, “Urban Climate Spatial and temporal air temperature variability in Berlin , Germany , during the years 2001 – 2010,” *Urban Clim.*, vol. 10, pp. 308–331, 2014, doi: 10.1016/j.uclim.2014.02.004.
- [66] Y. Y. Li, H. Zhang, and W. Kainz, “Monitoring patterns of urban heat islands of the fast-growing Shanghai metropolis, China: Using time-series of Landsat TM/ETM+ data,” *Int. J. Appl. Earth Obs. Geoinf.*, vol. 19, no. 1, pp. 127–138, 2012, doi: 10.1016/j.jag.2012.05.001.
- [67] I. D. Stewart, T. R. Oke, and E. S. Krayenhoff, “Evaluation of the ‘local climate zone’ scheme using temperature observations and model simulations,” *Int. J. Climatol.*, vol. 34, no. 4, pp. 1062–1080, 2014, doi: 10.1002/joc.3746.
- [68] A. Buyantuyev and J. Wu, “Urban heat islands and landscape heterogeneity: Linking spatiotemporal variations in surface temperatures to land-cover and socioeconomic patterns,” *Landsc. Ecol.*, vol. 25, no. 1, pp. 17–33, 2010, doi: 10.1007/s10980-009-9402-4.
- [69] J. Geletí, M. Lehnert, and P. Dobrovolný, “Land Surface Temperature Differences within Local Climate Zones , Based on Two Central European Cities,” *Remote Sens.*, pp. 1–18, 2016, doi: 10.3390/rs8100788.
- [70] M. Unal Cilek and A. Cilek, “Analyses of land surface temperature (LST) variability among local climate zones (LCZs) comparing Landsat-8 and ENVI-met model data,” *Sustain. Cities*

- Soc.*, vol. 69, no. October 2020, p. 102877, 2021, doi: 10.1016/j.scs.2021.102877.
- [71] W. Lin, T. Yu, X. Chang, W. Wu, and Y. Zhang, “Calculating cooling extents of green parks using remote sensing: Method and test,” *Landsc. Urban Plan.*, vol. 134, pp. 66–75, 2015, doi: 10.1016/j.landurbplan.2014.10.012.
- [72] Z. Yu, X. Guo, G. Jørgensen, and H. Vejre, “How can urban green spaces be planned for climate adaptation in subtropical cities?,” *Ecol. Indic.*, vol. 82, no. March, pp. 152–162, 2017, doi: 10.1016/j.ecolind.2017.07.002.
- [73] H. Du, W. Cai, Y. Xu, Z. Wang, Y. Wang, and Y. Cai, “Quantifying the cool island effects of urban green spaces using remote sensing Data,” *Urban For. Urban Green.*, vol. 27, no. February, pp. 24–31, 2017, doi: 10.1016/j.ufug.2017.06.008.
- [74] H. Xiao and Q. Weng, “The impact of land use and land cover changes on land surface temperature in a karst area of China,” *J. Environ. Manage.*, vol. 85, no. 1, pp. 245–257, 2007, doi: 10.1016/j.jenvman.2006.07.016.
- [75] R. C. Estoque, Y. Murayama, and S. W. Myint, “Effects of landscape composition and pattern on land surface temperature: An urban heat island study in the megacities of Southeast Asia,” *Sci. Total Environ.*, vol. 577, pp. 349–359, 2017, doi: 10.1016/j.scitotenv.2016.10.195.
- [76] Y. Xiang, C. Yuan, Q. Cen, C. Huang, and C. Wu, “Heat risk assessment and response to green infrastructure based on local climate zones,” vol. 248, no. November 2023, 2024.
- [77] Y. Luo, J. Yang, Q. Shi, Y. Xu, M. Menenti, and M. S. Wong, “Seasonal Cooling Effect of Vegetation and Albedo Applied to the LCZ Classification of Three Chinese Megacities,” *Remote Sens.*, vol. 15, no. 23, 2023, doi: 10.3390/rs15235478.
- [78] S. Shooshtarian and P. Rajagopalan, “Daytime thermal performance of different urban surfaces: a case study in educational institution precinct of Melbourne,” *Archit. Sci. Rev.*, vol. 61, no. 1–2, pp. 29–47, 2018, doi: 10.1080/00038628.2018.1432475.
- [79] A. M. Broadbent, A. M. Coutts, N. J. Tapper, and M. Demuzere, “The cooling effect of irrigation on urban microclimate during heatwave conditions,” *Urban Clim.*, vol. 23, pp. 309–329, 2018, doi: 10.1016/j.uclim.2017.05.002.
- [80] D. E. Bowler, L. Buyung-Ali, T. M. Knight, and A. S. Pullin, “Urban greening to cool towns and cities: A systematic review of the empirical evidence,” *Landsc. Urban Plan.*, vol. 97, no. 3, pp. 147–155, 2010, doi: 10.1016/j.landurbplan.2010.05.006.
- [81] A. S. M. S. Uddin, N. Khan, A. R. M. T. Islam, M. Kamruzzaman, and S. Shahid, “Changes in urbanization and urban heat island effect in Dhaka city,” *Theor. Appl. Climatol.*, vol. 147, no. 3–4, pp. 891–907, 2022, doi: 10.1007/s00704-021-03872-x.
- [82] B. Budhiraja, L. Gawuc, and G. Agrawal, “Seasonality of Surface Urban Heat Island in Delhi City Region Measured by Local Climate Zones and Conventional Indicators,” *IEEE J. Sel. Top. Appl. Earth Obs. Remote Sens.*, vol. 12, no. 12, pp. 5223–5232, 2019, doi: 10.1109/JSTARS.2019.2955133.

- [83] B. Bechtel *et al.*, “Urban Climate SUHI analysis using Local Climate Zones — A comparison of 50 cities,” *Urban Clim.*, vol. 28, no. January, p. 100451, 2019, doi: 10.1016/j.uclim.2019.01.005.
- [84] J. Quan, “Multi-Temporal Effects of Urban Forms and Functions on Urban Heat Islands Based on Local Climate Zone Classification,” pp. 9–11, 2019.
- [85] C. Dian, R. Pongrácz, Z. Dezső, and J. Bartholy, “Urban Climate Annual and monthly analysis of surface urban heat island intensity with respect to the local climate zones in Budapest,” *Urban Clim.*, vol. 31, no. December 2019, p. 100573, 2020, doi: 10.1016/j.uclim.2019.100573.
- [86] Y. Li, S. Schubert, J. P. Kropp, and D. Rybski, “On the influence of density and morphology on the Urban Heat Island intensity,” *Nat. Commun.*, vol. 11, no. 1, pp. 1–9, 2020, doi: 10.1038/s41467-020-16461-9.
- [87] C. B. Koc, P. Osmond, A. Peters, and M. Irger, “Understanding Land Surface Temperature Differences of Local Climate Zones Based on Airborne Remote Sensing Data,” *IEEE J. Sel. Top. Appl. Earth Obs. Remote Sens.*, vol. 11, no. 8, pp. 2724–2730, 2018, doi: 10.1109/JSTARS.2018.2815004.
- [88] Q. Jinling, “Enhanced geographic information system-based mapping of local climate zones in Beijing , China,” vol. 62, no. 12, pp. 2243–2260, 2019.
- [89] R. Giridharan and R. Emmanuel, “The impact of urban compactness , comfort strategies and energy consumption on tropical urban heat island intensity : A review,” *Sustain. Cities Soc.*, vol. 40, no. January, pp. 677–687, 2018, doi: 10.1016/j.scs.2018.01.024.

Author Statement

Author order	Author name	CRedit role(s)
1	Tania Sharmin	Conceptualization; Data curation; Formal analysis; Funding acquisition; Investigation; Methodology; Project administration; Resources; Software; Validation; Visualization; Roles/Writing - original draft; Writing - review & editing.
2	Adrian Chappell	Validation; Writing - review & editing.



Graphical abstract

Journal Pre-proof